Palaeogeography, Palaeoclimatology, Palaeoecology 679 (2025) 113267

Contents lists available at ScienceDirect

Palaeogeography, Palaeoclimatology, Palaeoecology

journal homepage: www.elsevier.com/locate/palaeo

Spatiotemporal evolution of an Early Jurassic erg in southern Africa (Clarens Formation, Karoo Supergroup)

Howard V. Head *, Emese M. Bordy

Department of Geological Sciences, University of Cape Town, Rondebosch, South Africa

ARTICLE INFO

Editor: Howard Falcon-Lang

Keywords:
Early Jurassic
Aeolian facies
Clarens Formation
Fluvial-aeolian interaction
Southern Africa

ABSTRACT

The Early Jurassic featured extensive global desert systems that are exemplified in southern Africa by the Lower Jurassic Clarens Formation, the youngest sedimentary unit of the Karoo Supergroup. This Sinemurian to Pliensbachian formation consists of thick massive sandstone beds and large-scale cross-bedded sandstones in its middle sections. Lenticular siltstones in the lower and upper parts suggest intermittent wet conditions. These vertical facies changes correspond to three, long- established stratigraphic zones, yet their palaeoenvironmental context within Early Jurassic Pangaean climate remains unclear.

Field data show that massive structureless deposits (68 %) and aeolian dune deposits (20 %) dominate the formation, with minor ephemeral channel, sand sheet, and pluvial deposits. Unconfined fluvial and debris flow deposits are least common. During semi-arid phases, limited sediment availability and higher moisture restricted dunes to isolated fields and resulted in significant downwind loess plains and fluvial incursions from the basin's southern and eastern margins. In contrast, aridification increased sand-size sediment supply, expanding the dune field into a sand sea and displacing the marginal erg facies eastward.

These spatiotemporal facies shifts in southern Pangaea align with a wet-dry-wet megacycle documented along the Tethyan margin in the north during the Sinemurian and Pliensbachian. The facies shifts are interpreted as indicators of global climatic influences on local sedimentation. The well-preserved aeolianites of the Clarens Formation provide key insights into ancient erg dynamics and modern dryland responses to global climate change.

1. Introduction

Long-term climatic and tectonic drivers exert an important control on the development of aeolian sedimentary systems and their preservation in the rock record, and thus, ancient sedimentary deposits can reflect the spatiotemporal variations in these geological drivers. Climatic cyclicity has been documented in the Lower Jurassic Clarens Formation of southern Africa (Figs. 1, 2). This formation is interpreted as an aeolian deposit characterized by complex interactions amongst aeolian, fluvial, and lacustrine processes in a vast desert setting (Du Toit, 1905; Van Eeden, 1937; Stockley, 1947; Beukes, 1969, 1970; Eriksson, 1981, 1986; Bordy and Catuneanu, 2001; Holzförster, 2007; Bordy and Head, 2018; Head and Bordy, 2023a, 2023b; Head et al., 2024).The most extensive work on this aeolian succession has been conducted by Beukes (1969, 1970), who interpreted a wet-dry-wet climate megacycle during the deposition of the Clarens Formation. Further research on the lacustrine and fluvial deposits identified by Beukes (1970) and Eriksson (1981, 1986) has been carried out by Head and Bordy (2023a).

This study focuses on evaluating the sedimentary facies and their association within the Clarens Formation to refine its spatiotemporal relationships, distribution, and geological controls within this ancient erg system. This well-preserved aeolian succession does not only contextualises the climate of southern Pangaea (i.e., southwestern Gondwana) within the global Early Jurassic, but also provides important evidence towards the understanding of past Earth systems behaviour and its implications for equivalent modern dryland environments and ecosystems.

2. Geological background

The Lower Jurassic Clarens Formation, along with the underlying Elliot and Molteno formations comprise the Stromberg Group of the Karoo Supergroup. It has a conformable relationship with both the underlying Elliot Formation and the overlying flood basalts of the

* Corresponding author.
E-mail address: hdxhow001@myuct.ac.za (H.V. Head).

https://doi.org/10.1016/j.palaeo.2025.113267
Received 18 June 2025; Received in revised form 5 September 2025; Accepted 5 September 2025
Available online 6 September 2025
0031-0182/© 2025 The Authors. Published by Elsevier B.V. This is an open access article under the CC BY license (http://creativecommons.org/licenses/by/4.0/).

Drakensberg Group, more specifically, that of the lower Barkly East Formation (Lock et al., 1974; Marsh and Eales, 1984; Moulin et al., 2011, 2017; Bordy et al., 2021). The lower contact with the Elliot Formation is a transitional interval of interbedded red beds and fine-grained pale sandstones, complicating the mapping of this gradational contact — see explanation in Bordy and Head (2018). The upper contact is sharp, undulates and is identified by the first appearance of extrusive volcanics associated with the Drakensberg Group (Beukes, 1970; Eriksson, 1981; Bordy and Head, 2018). Sandstone interbeds with a similar lithology to that of the Clarens Formation appear amongst the Barkly East Formation, suggesting continued sedimentation in between phases of early lava extrusion.

The Clarens Formation has an average thickness of 90 to 150 m across most of the outcrop area. Dramatic thickness fluctuations are particularly abundant in the south, where the largest thickness of over 300 m occurs (between Barkly East and Elliot), whereas the succession is completely missing in some locations (Du Toit, 1904, 1905, 1910; Beukes, 1969, 1970; Robinson et al., 1969; Johnson, 1976; Holzförster, 2007). In the northern outcrop area, a more subdued thickness variation is typical (Beukes, 1969, 1970; Eriksson, 1981, 1986; Bordy and Head, 2018). These south to north thickness changes are consistent with the tectonic setting of the main Karoo Basin (MKB; Fig. 1) during the final phases of its evolution.

Accumulation space in the basin has been widely accepted to have been created by flexural tectonics in a foreland system in response to subduction of the palaeo-Pacific plate along the Panthalassan margin of Gondwana (Catuneanu et al., 1998, 2005). The MKB is, therefore, considered a retro-arc foreland basin (Cole, 1992; Catuneanu et al., 1998, 2005). In this context, the smaller extent of the MKB during the deposition of the Stromberg Group (Figs. 1, 2) is attributed to foresag subsidence during the orogenic unloading in the Cape Fold Belt (Bordy et al., 2004a,b, 2005; Hanson et al., 2009). This unloading also resulted in the upliftment and erosion of the pre-Stormberg units on a regional scale (Bordy et al., 2004b). Foresag sedimentation was subsequently terminated by volcanism associated with the Karoo-Ferrar Large Igneous Province that was followed by the break-up of Gondwana (Beukes, 1970; Eriksson, 1981; Duncan et al., 1997; McClintock et al., 2008; Bordy and Head, 2018; Muir et al., 2020).

Beukes (1969, 1970), based on a regional study, classified three stratigraphic zones within the Clarens Formation, a lower and an upper zone where massive sandstones dominate the succession, and a middle zone where very large- to large-scale, cross-bedded sandstones become dominant over massive sandstones (Zone 1 to 3, respectively). In addition to the massive nature of zones 1 and 3, sedimentary features indicative of shallow water processes is also diagnostic for these zones, but never studied in detail. For this reason, the zonation was simply ascribed to a wet-dry-wet climatic megacycle (Beukes, 1969, 1970; Bordy and Head, 2018).

For the eastern outcrop area along the KwaZulu-Natal Drakensberg, Eriksson (1979, 1981, 1986) documented the occurrence of facies related to wadi channel and alluvial fan processes amongst the aeolian processes. These features were ascribed to a spatial component in the palaeoenvironment of the Clarens Formation, where the erg centre was dominated by large-scale, cross-bedded sandstones, with a wet aeolian system along the erg margin preserved in the eastern outcrop area. The documentation of freshwater fish (*Semionotus capensis),* crocodylomorphs (*Notochampsa istedana*), plant fragments, and petrified tree trunks (Broom, 1904; Du Toit, 1904; Haughton, 1924; Stockley, 1947; Meijs, 1960; Jubb, 1973; Forey and Gardiner, 1973; Bordy and Catuneanu, 2001, 2002; Bamford, 2004; Bordy et al., 2021; Dollman et al., 2021) supports the interpretation of episodic wet phases suggesting that the palaeoenvironment may not have been as harsh as initially interpreted (Bordy and Head, 2018; Head and Bordy, 2023a, 2023b). Moreover, field evidence presented by Bordy et al. (2020, 2021, 2023) suggest that localised ecosystems continued to thrive on the Clarens landscape during the initiation of volcanism at the turn of the Pliensbachian-Toarcian eruptive episode within the Karoo-Ferrar Large Igneous Province.

The Clarens erg system covered an enormous area of southern Gondwana during the Early Jurassic (Bordy and Head, 2018). Its stratigraphic equivalents are present in numerous Karoo-aged basins extending north of the MKB all the way to Zambia (Fig. 1A). Across southern Africa, these correlatives are represented by the Forest Sandstone Formation in Zimbabwe and Zambia, the Ntane and Bodibeng

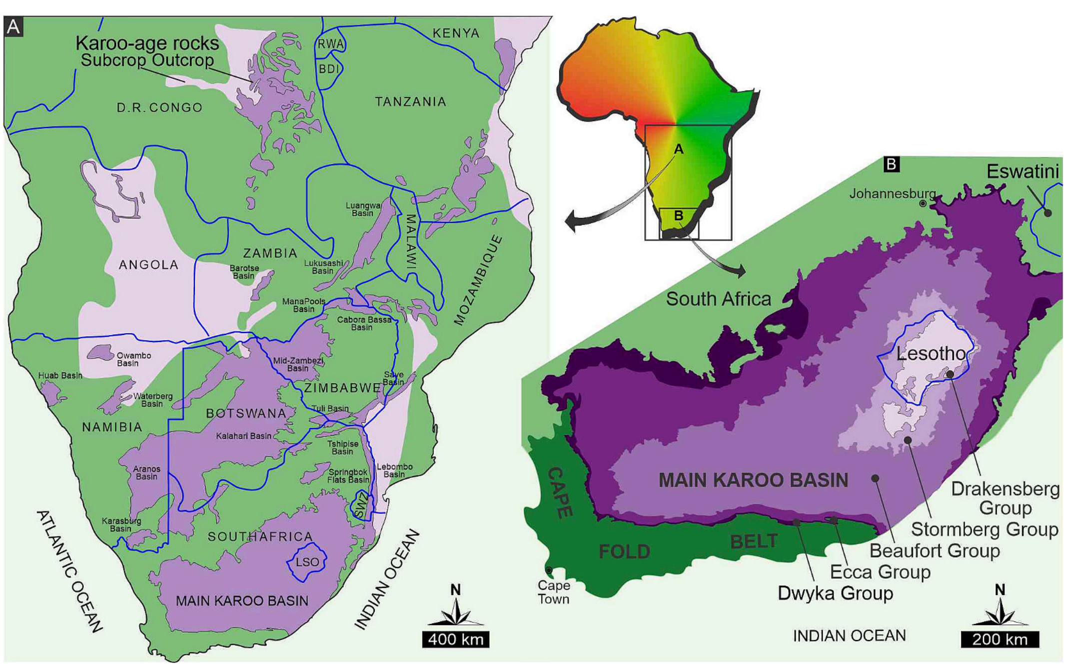

Fig. 1. Geological context of the Clarens Formation as part of Karoo-aged basins in Africa south of the equator. **A.** Karoo-aged basins in the southern half of Africa, where remnants of Clarens-equivalents may be preserved (also see Bordy and Head, 2018). **B.** Simplified geological map of the main Karoo Basin, illustrating the erosional remnant of the upper Karoo (Stormberg and Drakensberg Groups) in South Africa and Lesotho. Maps modified from Veevers et al. (1994). See Fig. 2 for study locations in and around Lesotho.

Sandstone Formations in Botswana, and the Etjo and Nkalatlou Formations in Namibia (Veevers et al., 1994; Johnson et al., 1996). Geological evidence indicates that the active Clarens erg was significantly larger than its *preserved* patchy outcrop region within the MKB (e.g., Veevers et al., 1994; Hanson et al., 2009). Therefore, the spatial distribution of the Clarens equivalent outcrops, spanning approximately 2000 km north-south and 1600 km east-west, suggests an active erg covering an area of about 3.2 × 10ˆ6 km^2. This implies an ancient sand sea roughly 1.4 times larger than the largest sand-covered surface area in the Sahara Desert and about 5 times larger than the northern Pangaean Early Jurassic Navajo Sand Sea, with an inferred original extent of approximately 6.25 × 10ˆ5 km^2 (Kocurek, 2003).

3. Methods

Sedimentological field work was conducted across the MKB of southern Africa, where outcrops of the Clarens Formation (Fig. 1A) were analysed for grain size, sedimentary structures, composition, lithology, and under- and overlying facies-contact types in combination with the measurement of detailed centimetre-scale sedimentary logs. This is based on the well-established sedimentary facies analysis method delineated by Miall (1974a, b, 1985, 1996) and commonly applied in aeolian rock successions (e.g., Mountney and Howell, 2000; Mountney and Thompson, 2002; Mountney and Jagger, 2004; Mountney, 2006; Hassan et al., 2018). The hierarchy of surfaces from Hasiotis et al. (2021) was used to distinguish important bounding surfaces. Photo panels of large-scale outcrops were also constructed to document and understand the three-dimensional nature of the facies (Table 1), facies associations (Table 2) and their spatial relationships (Miall, 1996; Mountney, 2006). Palaeocurrents were measured from the foreset dip direction of well-developed large-scale cross-bedded sandstones to understand the Early Jurassic sediment distribution patterns across this part of southwestern Gondwana (High and Picard, 1974; Miall, 1974; Dasgupta, 2002; Miall, 2016).

Facies distribution over the outcrop area was documented in outcrop profiles and in 33 sedimentary logs (Fig. 1A). Using ©2021 Google Earth Pro software, facies maps showing the distribution and proportions of facies associations were generated by extracting facies association data from each sedimentary log both from this study, from Head and Bordy (2023b) and the re-interpreted logs from Beukes (1969) and Eriksson (1983)— see Head (2022). This process was repeated for each of the different stratigraphic zones of the Clarens Formation. Since the facies proportions were extracted from 2D sedimentary logs, they reflect semi-quantitative estimations for small areas, which may not be fully representative of the facies associations throughout the basin.

The thickness map of the Clarens Formation was generated from thickness data derived from this study and previous work (e.g., Du Toit, 1904, 1905; Stockley, 1947; Beukes, 1969; Robinson et al., 1969; Eriksson, 1983). The latter dataset was tested for quality using digital elevation (terrain) tool in ©2021 Google Earth Pro software. The cleaned-up (quality assured) thickness values were imported into QGIS and a 0.5 by 0.5-degree overlay block grid created as part of the estimation input, comma separated value (CSV) files. The thickness estimation was conducted with an ordinary kriging method using the *gstat* and *sp* packages in Rstudio (Pebesma, 2004; Pebesma and Bivand, 2005; Bivand et al., 2013; R Core Team, 2014).

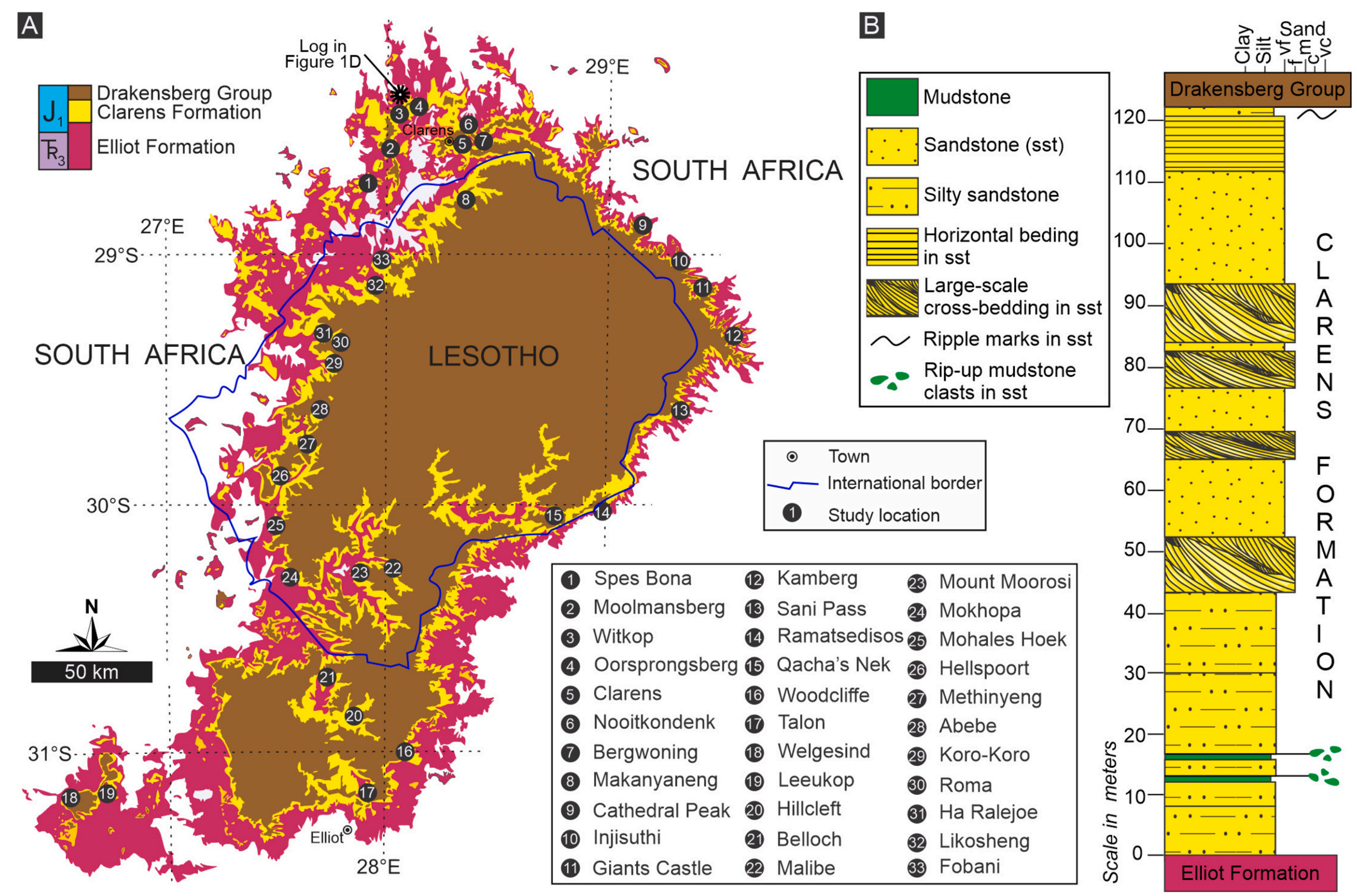

Fig. 2. Geological context of the Clarens Formation study sites within the main Karoo Basin in South Africa and Lesotho. **A.** Geological map of the upper Stormberg Group displaying 33 study locations. **B.** Representative sedimentary log of the Clarens Formation at Wonderkop in the eastern Free State (28°40′19.10"S; 27°41′55.76″E; also marked in Fig. 1A; see Bordy and Head, 2018). See Fig. 1 for regional context.

Table 1
Aeolian, fluvial, and lacustrine lithofacies in the Clarens Formation.

Code	Lithofacies	Description	Interpretation
Sse	Massive sandstone	Very fine- to silty sandstones/sandy siltstone; thick to very thick beds; fine sand to coarse silt grain size; same as facies three of Eriksson (1981, 1986).	Dust deposits (loess) or aeolian dune deposits without preserved internal structure
Ste	Large-scale, cross-bedded sandstone	Fine- to medium-grained sandstones; thick to very thick beds; same as facies four of Eriksson (1981, 1986)	Deposits of migrating aeolian dunes
Sle	Low-angle cross-bedded sandstone	Fine- to medium-grained sandstones; thick to very thick beds	Aeolian sand sheets or dune plinth deposits (translatent ripple stratification)
Sm	Massive sandstone	Fine- to medium grained sandstones; medium to thick beds, thin beds	Dune slumping or hyperconcentrated flow deposits distinguished from Sse by its grain size.
Sh	Horizontally laminated sandstone	Fine- to medium-grained sandstones; medium to thick beds	Upper flow regime flood deposits
Sl	Low-angle, cross-bedded sandstone	Fine- to medium-grained sandstones; often associated with Sh; thin beds	Upper flow regime flood deposits distinguished from Sle by its limited lateral extent.
Sp	Planar cross-bedded sandstone	Fine- to medium-grained sandstones; thick beds; Same as facies two of Eriksson (1981, 1986).	Lower flow regime, migration of channel bars
Sr	Ripple cross-laminated sandstone or ripple marked surfaces	Asymmetrical, symmetrical and interference ripples	Wave (bidirectional) and current (unidirectional) flow in a low-energy environment; changing hydrodynamic conditions indicated by interference ripples
Sw	Convolutely-laminated sandstone	Soft-sediment deformation of laminated sandstones; similar to facies one of Eriksson (1981, 1986)	Rapid deposition and high sediment load in ephemeral channels and sheetfloods
Sae	Wavy-laminated sandstone	Fine-grained sandstones; medium thick beds	Adhesion deposit that forms when dry sand clings to a damp surface
Fl	Laminated mudstone	Thin to thick beds; similar to facies one of Eriksson (1981, 1986)	Subaqueous settling of wind-blown sediment
Fm	Massive mudstone	Thin to thick beds; similar to facies one of Eriksson (1981, 1986)	Suspension settling from water column and wind derived material into lake, bioturbated
Gmc	Mudstone-clast conglomerate	Rip-up mudstone clasts in massive sandstone	Deposits from erosive, high-energy flow
B	Basalt	Basalt lenses in large-scale, cross-bedded sandstone	Basalt flow dammed in dune field
Ds	Desiccation cracks	Polygonal pattern of shallow fissures often filled with sandstones; associated with Sr	Drying of the wet sediment layer

4. Results

4.1. Facies

The facies types in the Clarens Formation have been discussed by Eriksson (1981, 1983, 1986) based on studies conducted in the KwaZulu-Natal Drakensberg region (Fig. 1). Eriksson (1981, 1986) defined four facies types: 1) a laminated, fine-grained, convoluted sandstone unit that is interbedded with mudstones and very fine-grained sandstones having a lacustrine origin associated with sheetflood deposits; 2) a medium- to coarse-grained cross-stratified sandstone unit that reflects the deposits of desert flood-related braided-wadi channels and sheet flooding; 3) a massive sandstone unit formed in mass-movement processes linked to flooding events, and 4) a very large- to large-scale cross-bedded sandstone that formed by dune migration. In this regional study of the Clarens Formation, 15 lithofacies and seven distinctive facies associations are defined (Tables 1 and 2), and are, in part, consistent with the four facies types of Eriksson (1981, 1986).

Table 2
Aeolian, fluvial, and lacustrine lithofacies associations in the Clarens Formation.

Facies association	Lithofacies	Diagnostic features	Depositional process
FA 1	Ste, Sle	Very large to large-scale cross-bedded sandstones; medium to fine-grained sand	Migrating dunes; dune plinth deposits
FA 2	Sse	Structureless sandstones; very fine sand to coarse silt grain size, laterally extensive	Aeolian dust, suspension fallout
FA 3	Sle, ste	horizontally stratified and low-angle cross-bedded sandstones; Fine – to very fine-grained sand	Migrating wind ripples/ sand sheets with subordinate small-scale dunes
FA 4	Sh, Sp, Sw, Gmc	Lenticular, laterally extensive, planar cross-bedded sandstones; basal mud clast conglomerate; coarse to medium grained	Channel fill
FA 5	Sm, Sh, Sl, Sr	Massive to horizontally stratified sandstones; transitioning to low-angle and ripple cross-laminated sandstones, tabular	Unconfined flow
FA 6	Fm, Fl, Sm	Laminated/massive mudstones, lenticular to laterally extensive	Settling of mud from water column.
FA 7	Gm, Sm	Massive sandstone to conglomerate; basalt clasts	Hyperconcentrated flows/debris flow

4.1.1. Facies association 1 (FA 1)

4.1.1.1. Description. This facies association comprises very fine- to medium-grained, pale orange to off-white sandstones that are well-sorted and arranged in trough cross-bedded sets (Ste – Fig. 3) with a sharp lower and upper bounding surface (Fig. 3A–C). Laterally extensive, tabular packages appear throughout the basin. Within these, individual sets range in thickness from 0.5 to 2 m, whereas multiple stacked sets have thicknesses of roughly 2 to 10 m with extreme thicknesses of up to 40 m also recorded in places. Two internal arrangement patterns can be identified: 1) abundant occurrences of massive sandstone wedges that thin downslope and varies in thickness from 2 to 8 cm; (Fig. 5A, B) and 2) millimetre-scale sandstone laminae packages that appear to thicken upslope (Fig. 5A, B) with a set thickness range of 5 to 30 cm. Cross-beds are tangential towards the bed bottom (Fig. 3C) and may in places truncate onto basal sandstones to form bedset deviation surfaces (Figs. 2B, C). In parts, low-angle, cross-bedded sandstones (Sle) also appear interbedded with large-scale, cross-bedded sandstones (Ste – Fig. 3D). Although Facies Association 1 is identified throughout the basin, key sites where it is well preserved are at Balloch, Sani Pass, Koro-Koro and Likosheng (Figs. 1–4). The most comprehensive exposure of very large- to large-scale, cross-bedded sandstones is preserved at

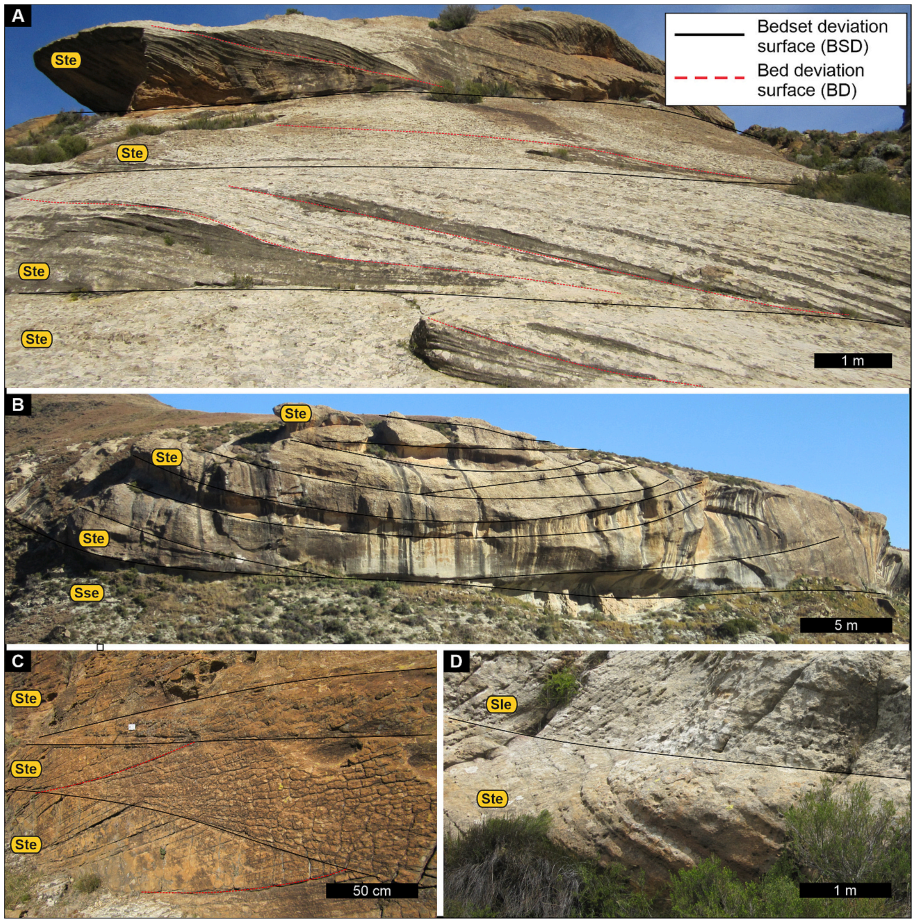

Fig. 3. Facies Association 1. **A.** Large-scale cross-bedded sandstone co-sets at Balloch with reactivation surfaces marked in red dotted line. **B.** Large-scale, cross-bedded sandstone cosets in cross sectional view (W-E) close to Hillcleft. **C.** Large-scale, cross-bedded sandstone with erosional contacts at Koro-Koro. Note the tangential nature of the foresets towards the bottom contact. **D.** Large-scale, cross-bedded sandstone associated with low-angle, cross-bedded sandstone at Witkop. See Table 1 for facies description and Fig. 2 for site locations. Bounding surface hierarchy from Hasiotis et al., 2021. (For interpretation of the references to colour in this figure legend, the reader is referred to the web version of this article.)

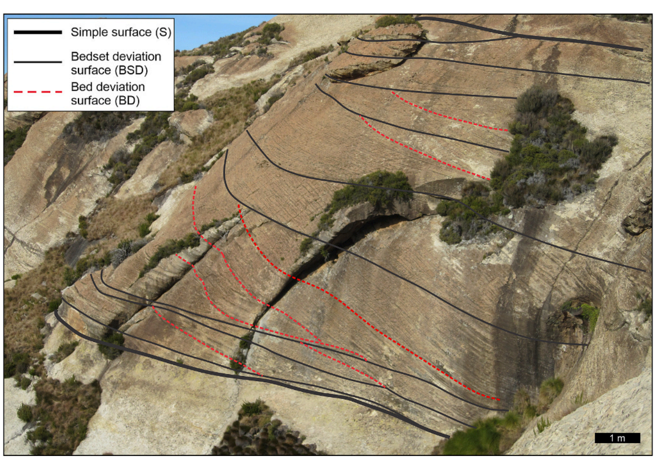

Fig. 4. Bounding surface arrangements in Facies Association 1 at Balloch. For site location, see Fig. 1. Bounding surface hierarchy based on Hasiotis et al., 2021.

Balloch, where bedset deviation surfaces are particularly abundant (Fig. 4). At Methinyeng, large-scale, cross-bedded sandstones are interbedded with lenses of basalt (Fig. 1, 6A–D) and can be shown to form a continuous lava body where the lenses (Figs. 15B and D) represent extensions of the main lava flow. A ropey texture is preserved on the baked lower contact with the massive sandstone (Fig. 6C) that contains charcoalified plant and wood fragments. These isolated basalt bodies are overlain by horizontal to low-angle, cross-bedded sandstones.

4.1.1.2. Interpretation. Very large- to large-scale, cross-bedded sandstones (Ste), along with the associated low-angle, cross-bedded sandstones (Sle), suggest that the facies association resulted from migrating dunes (Kocurek and Dott, 1981; Mountney, 2006). The internal stacking arrangement of the sandstones as laminated wedges and massive sandstone wedges represent translatent ripple stratification and grainflow strata that are typical of dune slip-face processes (Hunter, 1977; Rubin and Hunter, 1982; Kocurek and Dott, 1981; Kocurek, 1991; Mountney, 2006). This type of aeolian stratification indicates the dominance of grainflow processes with interbedded tongues of translatent ripple stratification as described by Kocurek (1991). This is shown to represent alternating winds, where a transverse direction results in grainflow slipface advancement and an oblique or inverse wind direction that results in along slope lee-face transport (Rubin and Hunter, 1982; Kocurek, 1991; Crabaugh and Kocurek, 1993).

The laminated wedges could represent grainfall laminae (Hunter, 1977; Rubin and Hunter, 1982), however, its appearance as wedges that thicken towards the lower part of the cross-beds (Fig. 5A) is more consistent with a translatent ripple stratification interpretation. In addition, the dominant preservation of grainflow strata within large-scale, cross-bedded sandstones suggests that dunes were relatively large (Rubin and Hunter, 1982; Kocurek and Dott, 1981). A positive

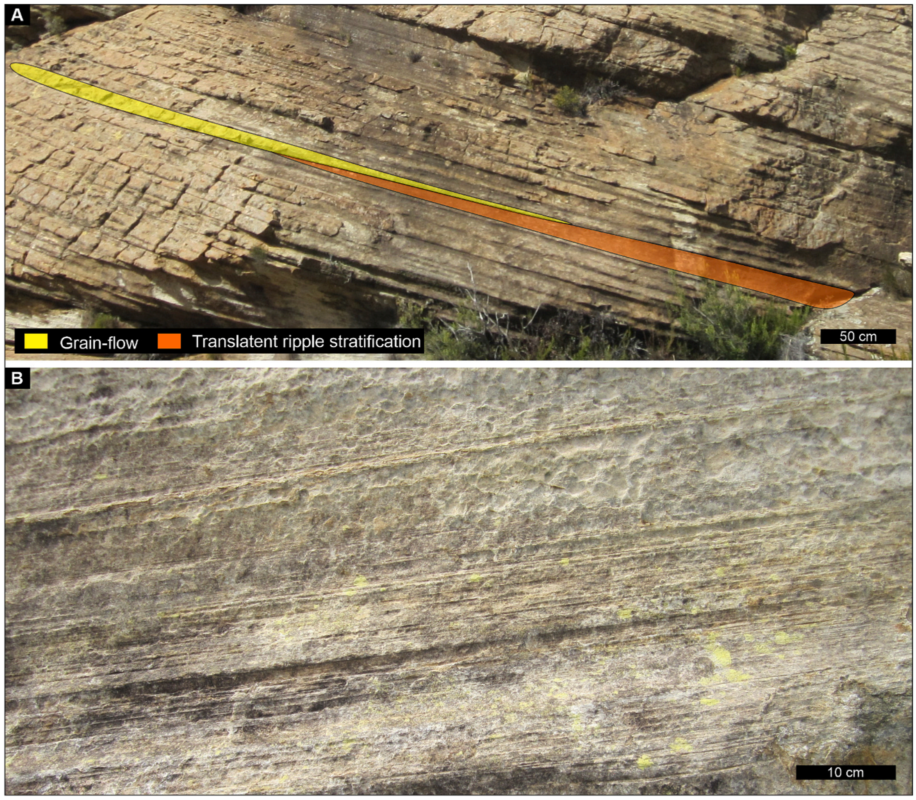

Fig. 5. Aeolian dune stacking arrangement within large-scale cross-bedded sandstones in the in Facies Association 1. **A.** Overview of grainflow and translatent ripple stratification that forms the foresets of large-scale cross-beds at Balloch. **B.** Close-up view of translatent ripple stratification interbedded with wedges of massive grainflow strata at Roma. For site locations, see Fig. 2.

correlation between dune height and grainflow thickness has also been described (e.g., Hunter, 1977; Kocurek and Dott, 1981), which also supports a large dune height for dunes of the Clarens Formation. The low-angle, cross-bedded sandstones found amongst the cross-bedded sandstones can be related to dune plinth deposits as dunes migrate over one another and fill dune hollows (Hunter, 1977; Rubin and Hunter, 1982; Kocurek and Havholm, 1993; Mountney, 2006). These dune plinth deposits result from wind ripple lamination that form on dunes with low to moderate inclinations (Mountney, 2006). The abundance of reactivation surfaces along with the observed foreset stacking arrangement indicates that the wind regime may not have been unimodal and prone to wind reversals (Hunter, 1981; Kocurek, 1991; Kocurek and Day, 2018). The abundance of bedset deviation surfaces at Balloch further suggests the development of compound draa in this area and represents the superimposition of smaller dunes along draa flanks (Mountney, 2006, Hasiotis et al., 2021).

The geometry of the basalt bodies within the large-scale, cross-bedded sandstones (Ste) in the uppermost Clarens Formation show that the lava flowed into an active dune field, where aeolian bedforms controlled the lava flow direction (cf. Jerram et al., 2000). The charred plant and wood fragments further suggest that the interdunes may have contained small ponds with trees and plants. Moreover, the presence of these bodies implies that the aeolian system was still active during the initial stages of lava extrusion as part of a coeval interfingering relationship. Therefore, these basalt lenses are not true lenses, but rather extensions of basalt flows where the outcrop orientation does not allow for the observation of the entire flow.

Moreover, the low-angle, cross-bedded sandstone (Sl) overlying the basalt lenses (B) could suggest that sediment availability was influenced by the lava flows, as sand sheets (Sle) are associated with limited sediment availability (Kocurek and Nielson, 1986). Jerram et al. (2000) show evidence that a change in bedform size during continuous lava flow deposition may corroborate such an interpretation, although here associated with the appearance of sand sheets rather than a change in bedform size. This facies association has been commonly described in the literature (e.g., Du Toit, 1904; Stockley, 1947; Beukes, 1969, 1970; Johnson, 1976; Eriksson, 1981, 1986; Bordy and Head, 2018), and has been linked with the informal zonation of the Clarens Formation by Beukes (1969, 1970) based on its abundant appearance sandwiched between the upper and a lower zone that are dominated by massive sandstones.

4.1.2. Facies Association 2 (FA 2)

4.1.2.1. Description. The Clarens Formation is dominated by massive sandstones that are laterally extensive (Fig. 7), thick to very thickly bedded (1 to 5 m with extremes of up to 15 m) and composed of very fine silty sand to sandy silt. Sandstones are moderately to well sorted and are light pink, green, cream to buff in colour. These structureless sandstones (Sse — Table 1) occur throughout the basin, mostly associated with the basal and upper parts of the Clarens Formation (Fig. 7A), although they are also locally interbedded with large-scale, cross-bedded sandstones and smaller scale siltstones (Fig. 7B). Characteristically, the massive sandstones appear very homogenous in outcrops (Fig. 7C) and as such, they were specifically investigated using sedimentary grain-size, grain shape and grain fabric trends to determine possible processes of deposition by Head and Bordy (2023b). Therefore, this facies association is not described in more detail herein.

4.1.2.2. Interpretation. Typically, Facies Association 2 in the Clarens Formation and elsewhere have been interpreted as dune slumping during intense rainstorms in modern and ancient aeolian systems (eg., Eriksson, 1983, 1986; Loope et al., 1998; Sweeney and Loope, 2001; Simpson et al., 2002; Heness et al., 2014). Based on grain characteristics

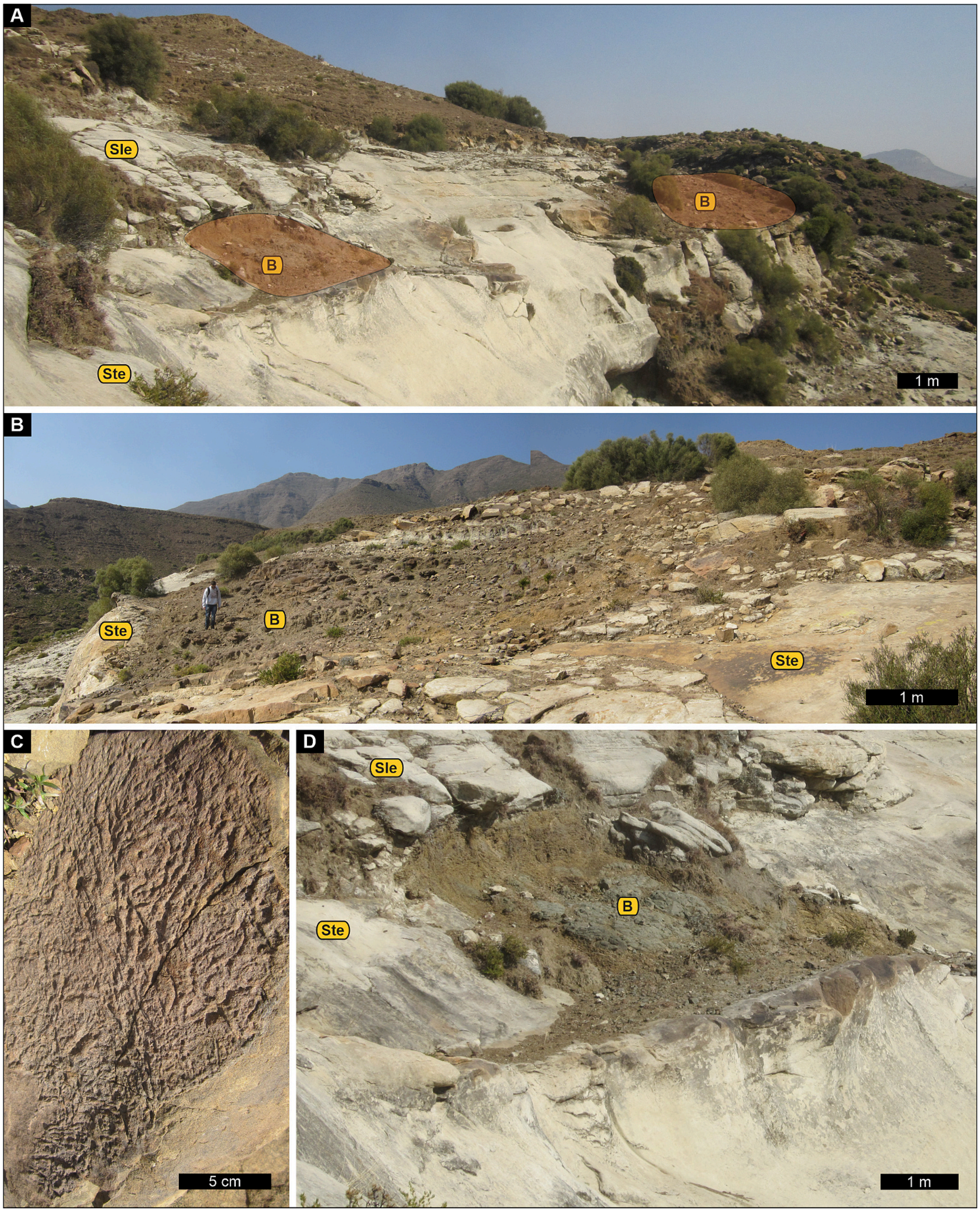

Fig. 6. Basalt interbedded with Facies Association 1 at Methinyeng. **A.** Large-scale, cross-bedded sandstones with interbedded lenses of basalt. **B.** Close-up view of the larger basalt lens. **C.** Baked basal surface of the basalt lens with ropey surface texture. **D.** Close-up view of the smaller basalt lens within large-scale, cross-bedded sandstone. See Table 1 for facies descriptions and Fig. 2 for site location.

investigated by Head and Bordy (2023b), the massive sandstones can be subdivided into six different facies types. These six massive deposit types represent a series of erg marginal to outer ergdepositional processes related to dune migration and dust storms in the dynamic, regional erg system in southwestern Gondwana due to local and regional Early Jurassic atmospheric circulation patterns (Head and Bordy, 2023a; Head and Bordy, 2023b; Vandenberghe, 2013). Although six depositional settings have been identified in the massive facies in the Clarens Formation, Head and Bordy (2023b) show that FA2 can dominantly be attributed to either a sandy loess or a classic loess deposit, and therefore FA2 is interpreted as dominantly dust depositional processes in short term to long term suspension during continuous and consistent dust storms.

4.1.3. *Facies Association 3 (FA 3)*

4.1.3.1. Description. Facies Association 3 occurs as horizontally laminated (Sh) to low-angle cross-bedded (Sl) facies in laterally continuous tabular sandstone bodies (Fig. 8). These sheet-like sandstones are very fine- to medium-grained and well sorted with a thickness that ranges between 0.5 and 5 m, although extreme thicknesses of up to 10 m are recorded in parts. Individual laminae are 2 to 4 mm, and in parts appear to be interbedded with massive wedges (Fig. 8B). Upper and lower contacts appear as mostly sharp horizontal to less abundant undulating surfaces. Cross-bedded sandstones (Ste) are also locally present (Fig. 8C-D). Facies Association 3 has been identified at Leeuwkop, Sani Pass, Kamberg, Hellspoort, Ramatsediso's Nek and Balloch (Fig. 1), and Beukes (1969) also recorded them in his sedimentary logs.

Fig. 7. Facies Association 2. **A**. Massive deposits in the upper part of the Clarens Formation at Qachas Nek. **B**. Massive deposits with interbedded siltstone. **C**. Massive deposits from Cathedral Peak with stream-cut potholes.

4.1.3.2. Interpretation. Sets of horizontally stratified (Sh) and low-angle, cross-bedded sandstones (Sl) are the expression of aeolian sand sheets that come about when wind ripples migrate and climb in a dry aeolian setting (Hunter, 1977; Kocurek and Nielson, 1986; Mountney, 2006; do Amarante et al., 2019). The internal structure of the wind ripples is often not distinguishable due to the uniformity of the grainsize within the deposit (Mountney, 2006), and the preservation of sandstone laminae may indicate that Facies Association 3 is composed of sub critically climbing translatent ripple strata (Hunter, 1977; Kocurek, 1991), whereas the interbedded massive sandstone wedges may reflect laminated sandstones in which the structures are obscured by weathering. The formation of aeolian sand sheets require very specific conditions and they usually form where dune formation is inhibited, typically during times of limited sediment availability related to increased moisture (Kocurek and Nielson, 1986). Sand sheets in modern desert settings are frequently associated with erg borders or underlie deserts (Mountney, 2006).

Similarly, thick sand sheet deposits within the Clarens Formation mostly developed close to erg margins and may have been associated with the leading edge (fore erg) or trailing margin (back erg) of the aeolian system (Kocurek and Nielson, 1986; Porter, 1986, 1987; Langford and Chan, 1993; Cosgrove et al., 2021a, 2021b). In addition, sand sheets showing planar surfaces have also been linked to a high water-table and may also be interbedded with cross-bedded sandstones (Kocurek and Nielson, 1986; Langford and Chan, 1993; Mountney, 2006). Such facies associations may develop in transitional zones such as areas where a change from fluvial to aeolian processes occur (Cain and Mountney, 2009). Evidence for this is seen at Balloch, where cross-bedded sandstones (Ste) are found interbedded with horizontally stratified (Sh) sandstones and represent the development of small-scale dunes amongst sand sheets (Kocurek and Dott, 1981; Kocurek and Nielson, 1986; Mountney, 2006; Trewin, 1993).

4.1.4. Facies Association 4 (FA 4)

4.1.4.1. Description. Facies Association 4 comprises stacked laterally extensive, lenticular to ribbon-like sandstone bodies consisting of very fine - to coarse-grained, gritty sandstone with thicknesses that vary between 0.5 and 1.5 m. Typically, horizontal stratification (Sh) and planar cross-bedded sandstones (Sp – Figs. 8B and 9A–B) are present and preserves soft-sediment deformation (recumbent cross-bedding) structures (Sw) throughout (Fig. 9C). Lenses of intraformational mudstone-clast conglomerates (Gmc) mark the bases of the sandstones (Fig. 9A–B), and rip-up mudstone clasts are also incorporated into basal parts of the channel-shaped sandstones (Fig. 10C). This facies association is best preserved at Kamberg and, to a lesser extent, at Ha Ralejoe and Woodcliffe. At Woodcliffe, ex-situ petrified wood fragments (Fig. 10D) were recorded a few m away from a cross-bedded sandstone (Sp) outcrop.

4.1.4.2. Interpretation. The combination of planar cross-bedded (Sp), horizontally stratified sandstones (Sh) and intraformational mudstones clasts conglomerates (Gmc) suggest that Facies Association 4 represents channel fill deposits, possibly in a low-sinuosity braided fluvial system (Miall, 1985; Hassan et al., 2018; Priddy and Clarke, 2020). Cross-bedded sets of sandstones suggest the migration of subaqueous channel bars, whereas the intraformational mudstone-clast conglomerate suggest high-energy conditions that reworked and cannibalised finer grained in-channel and/or over bank deposits (Hassan et al., 2018; Priddy and Clarke, 2020). The associated soft-sediment deformation (recumbent cross-bedding) reflects the strength of current drag that induced down slope gravitational slip during such high sediment load episodes (Allen and Banks, 1972; Hassan et al., 2018) and is characteristic of Facies Association 4. Furthermore, the sandy, highly mobile sediment surface was likely sparsely vegetated as suggested by the absence of palaeosols or in situ overbank fines (Cain and Mountney, 2009). This facies association was also described from the KwaZulu-Natal Drakensberg by Eriksson (1981, 1986) and was interpreted as

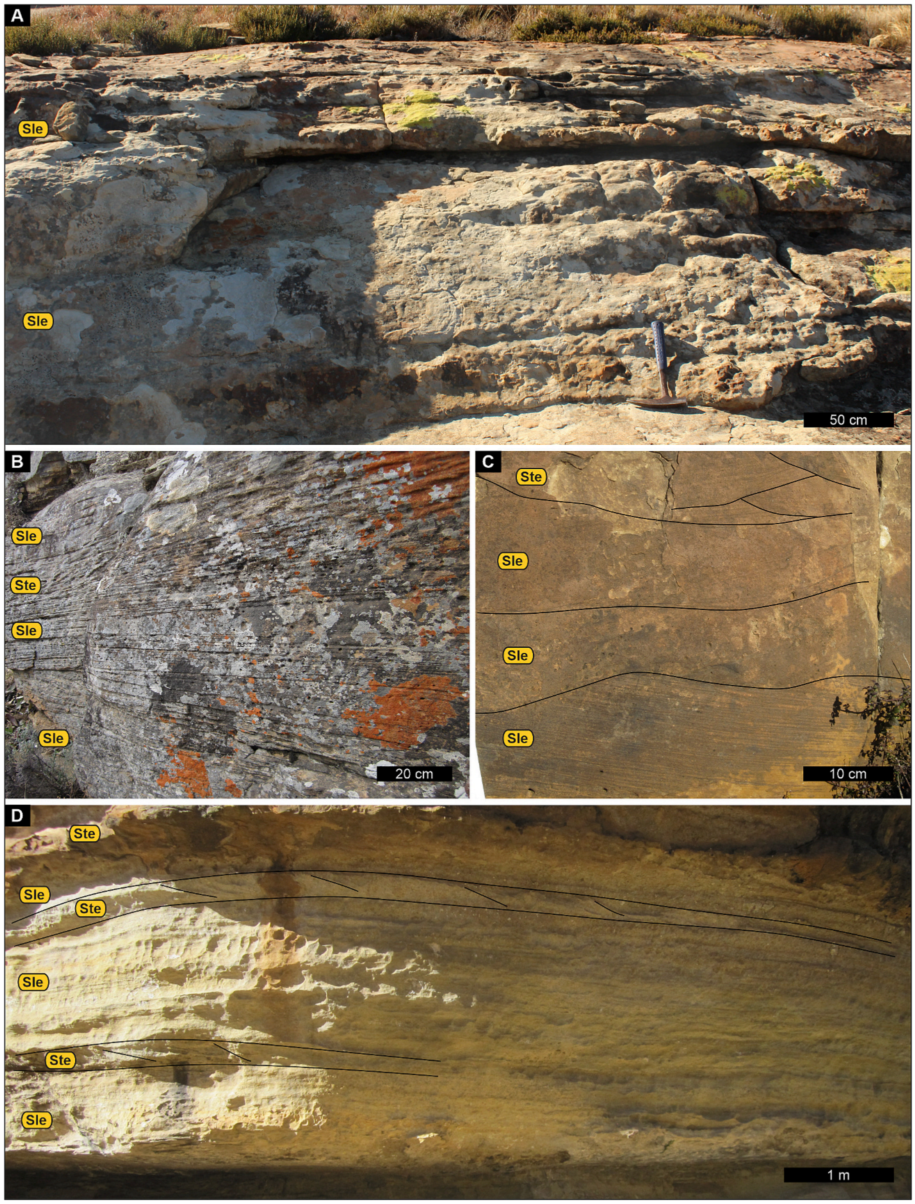

Fig. 8. Facies Association 3. **A**. Low-angle, cross-bedding at Ramatsediso's Nek. **B**. Low-angle, cross-bedding interbedded sandstone wedges and laminae at Kamberg. **C**. Low-angle, cross-bedding interbedded with small-scale cross-bedding at Hellspoort. **D**. Low-angle, cross-bedding grading into horizontal stratification and interbedded with small-scale cross-bedding at Balloch. See Table 1 for facies descriptions and Fig. 2 for site locations.

the product of wadi processes and distal alluvial fan systems that were situated in the south and the east of the basin.

4.1.5. Facies Association 5 (FA 5)

4.1.5.1. Description. Facies Association 5 comprise laterally extensive, tabular, white to light pink, very fine - to medium-grained sandstones with thicknesses varying between 0.5 and 1 m. Repeated cycles of massive (Sm – Fig. 11A), horizontal (Sh – Fig. 11B) and low-angle cross-bedded sandstones (Sl – Fig. 11C) are common. The Sm-Sh-Sl cycles transition into ripple cross-laminated (Sr – Fig. 11A and inset) sandstones that show ripple marks, and in places, are associated with desiccation cracks (Fig. 11D). This facies association is best preserved at Ramatsediso's Nek, Likosheng and Kamberg, occurring towards the upper contact with the Drakensberg Group, and has also been described in KwaZulu Natal (Eriksson, 1981; Eriksson, 1983; Eriksson, 1986; van Dijk and Eriksson, 2021).

4.1.5.2. Interpretation. Association of massive (Sm), horizontally stratified (Sh), low-angle, cross-bedded (Sl) and ripple cross-laminated (Sr) sandstones are interpreted as poorly confined to unconfined subaqueous sand sheets of fluvial origin (Hampton and Horton, 2007, North and Davidson, 2012; Pérez Mayoral et al., 2021). Horizontal stratification suggests upper flow regime conditions that was short-lived resulting in sheetlike geometries (McKee, 1966). The transition from horizontal to low-angle, cross-bedding indicates changes in flow energy, while ripple-cross lamination and the occurrence of ripple marks on upper bedding planes suggest waning flow conditions associated with termination of flow (Hampton and Horton, 2007). These sedimentary features are representative of deposition within wide, ephemeral streams with initial upper flow regime conditions (McKee, 1966; Mountney, 2006). Massive sandstones may be related to deposition of hyperconcentrated flows during periods of high rainfall (Priddy and Clarke, 2020). In some localities, these are extensively preserved, such as Kamberg, where it may represent amalgamated channel-forms resulting from long-lasting confined runoff during frequent precipitation/flooding events (ACF of

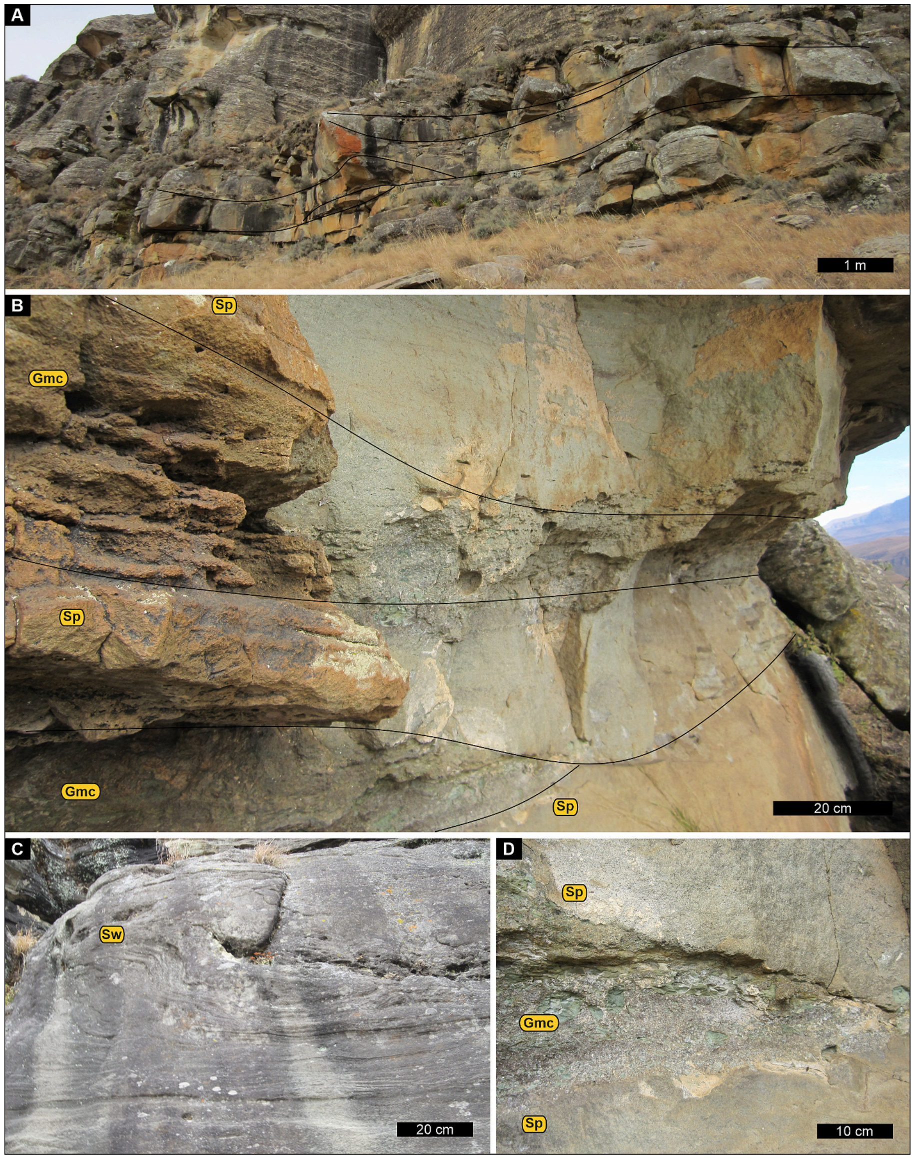

Fig. 9. Facies Association 4 at Kamberg. **A.** Multi-storey channel feature in the lower succession. **B.** Close-up view of the basal cross-bedded sandstones with conglomerate lenses. **C.** Soft-sediment deformation structure. **D.** Conglomerate lens in planar cross-bedded sandstones; note the rip-up mudstone clasts that indicate reworking. See Table 1 for facies descriptions and Fig. 2 for site location.

Hême de Lacotte and Mountney, 2022).

4.1.6. Facies Association 6 (FA 6)

4.1.6.1. Description. The components of Facies Association 6 comprise lenticular to laterally extensive tabular green to dark grey laminated (Fl – Fig. 12A, B) to massive mudstones (Fm – Fig. 12C) that are ~0.5- to 40-m-thick. Wavy-laminated (Sae), horizontally stratified (Sh), low-angle, cross-bedded (Sl) to massive sandstones (Sm) are interbedded with the mudstones (see Head and Bordy, 2023a). The mudstones can be mapped over lateral distances of ~30 m to >5 km. They may laterally wedge out, onlapping to large-scale, cross-bedded (Ste – Fig. 12C) or massive sandstones (Sse). In parts, convoluted bedding is associated with the mudstones and load casts are common at the base of the overlying massive sandstones (Fig. 12A, B). The sandstones interbedded with the mudstones preserve a range of sedimentary structures: ripple marks, interference ripples, microbially influenced sedimentary structures (MISS), plant and charcoal fragments, rill marks, desiccation cracks, and bioturbation structures such as vertical burrows, possible snail trail or flying traces and vertebrate footprints. Additionally, various plant and wood fragments occur within or in close proximity to the lenticular mudstones. Pluvial deposits in the Clarens Formation have been investigated in Head and Bordy (2023a), and specifics relating to the spatial distribution, aeolian-lacustrine interaction and genesis are discussed therein.

4.1.6.2. Interpretation. Lenticular to laterally extensive mudstones represent deposition within small-scale ponds, to large-scale lakes, whereas convoluted beds and load casts indicate rapid burial while the sediments were still wet (Selker, 1993). Silt likely entered the water-bodies in two ways, from direct dust fall processes and, secondly, from lake margin processes that occurred on the lake edge (Mountney, 2006; Vandenberghe, 2013; Vandenberghe et al., 2018). Wavy-laminated sandstones (Sae) suggest adhesion lamination processes, where dry sand adheres to a damp surface typical in damp to wet interdune areas (Kocurek and Dott, 1981; Hummel and Kocurek, 1984; Mountney, 2006). The appearance of laterally extensive massive (Sm) sandstones with convoluted bedding represent flood-related hyperconcentrated

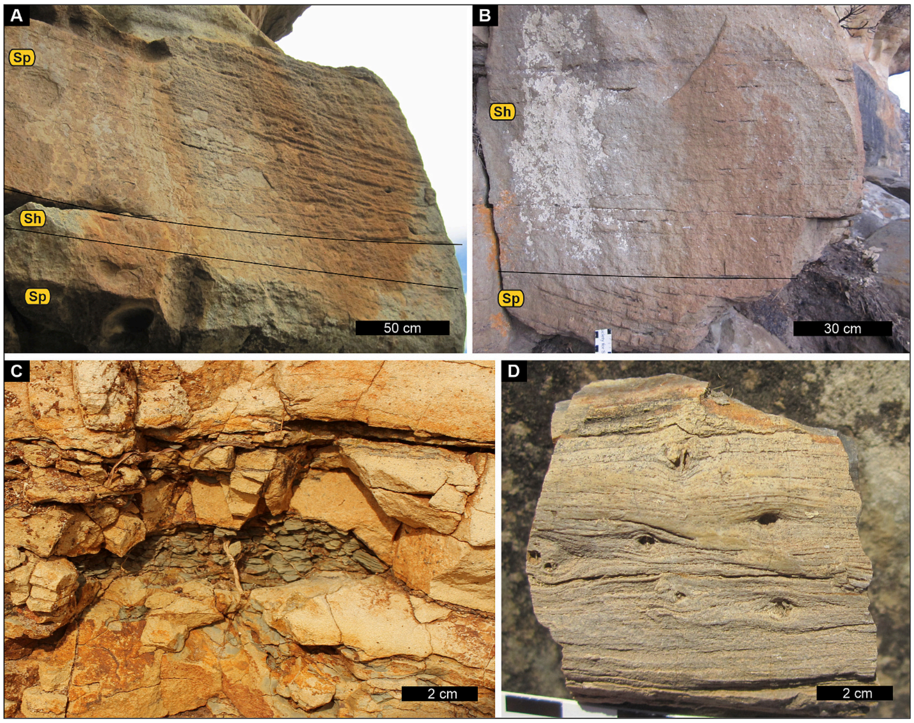

Fig. 10. Facies Association 4. **A.** Horizontally stratified sandstones typically occur amongst planar cross-bedded sandstones at Kamberg. **B.** Planar cross-bedded sandstones transitioning into horizontally stratified sandstones indicating decreasing energy. **C.** Close-up view of the rip-up mudstone clasts common within the basal part of cross-bedded sandstones at Ha Ralejoe. **D.** Ex-situ petrified wood fragment located near planar cross-bedded sandstone outcrops at Woodcliffe. See Table 1 for facies descriptions and Fig. 2 for site locations.

flows into interdunes and lakes (Svendsen et al., 2003, Priddy and Clarke, 2020). Moreover, rill marks, adhesion structures, possible snail trail or flying traces, and symmetrical ripple marks are all associated with lake margin processes during emergence of the sediments. Fossil fish (Fig. 12D) have also been identified within this facies association of the Clarens Formation (Haughton, 1924, Jubb, 1973 – Fig. 12D), although not documented in this study.

As shown in Head and Bordy (2023a), pluvial deposits (FA6) in the Clarens Formation are interpreted as products of: 1) meso-scale lakes (ponds according to Benavente and Bohacs, 2024) that form in interdune hollows, 2) macro-scale lakes (shallow lakes according to Benavente and Bohacs, 2024) with abundant lake marginal process preservation and 3) macro-scale lakes (shallow lakes according to Benavente and Bohacs, 2024) where interdunes were large enough to develop flood-related hyperconcentrated flows. The development of these different lake settings was a function of both the physical distance from the erg margin and the available accumulation space (Head and Bordy, 2023a). In the north of the basin, which is representative of the erg centre, lake sizes were limited by migrating dunes, where ponds formed in interdune hollows. In the south of the basin, closer to the erg margin, meso- and macro-scale lakes developed due to the reworking of dunes as the interdune expanded as a function of episodic water table rises (Head and Bordy, 2023a). Additionally, lacustrine facies in the south of the basin also developed thicker deposits, attributed to higher degrees of accumulation space creation as a result of faster subsidence rates. These lacustrine facies primarily appear in the lower part of the succession.

4.1.7. Facies Association 7 (FA 7)

4.1.7.1. Description. This facies association is characterized by lenticular, massive to crudely stratified, dark brown to grey sandstones (Sm) with basalt pebbles and massive, matrix-supported conglomerates (Gm). These facies are also associated with very fine-grained massive silty sandstones (Sse) and horizontally stratified (Sh), low-angle, cross-bedded (Sl) and ripple cross-laminated (Sr) sandstones. It is rarely observed across the basin. In places, plant impressions and charred plant fragments are present (Fig. 13D).

4.1.7.2. Interpretation. Lenticular, massive sandstones (Sm) associated with massive conglomerates (Gmc) are interpreted as a debris-flow or hyperconcentrated-flow deposits generated by flash floods within the erg. Given the dark colour and the inclusion of basalt pebbles in Facies Association 7, a nearby basalt source is highly likely. Debris-flow deposits and reworked basaltic material incorporated into the uppermost Clarens Formation have also been discussed by Bordy et al. (2021); see their Figs. 3, 4, 5).

4.2. The upper contact of the Clarens Formation

4.2.1.1. Description. Typically, the contact undulates with an amplitude of 2.5 m (Fig. 14D) and shows evidence of lava baking and preservation features (e.g., ropey texture - Fig. 14A, C), wind ripple marks (Fig. 14A), desiccation cracks (Fig. 15A) and striations (Fig. 14C). In parts, basalt lenses occur within sandstones, while at Mount Moorosi, a sandstone interbed within the basalts has an onlapping relationship with the youngest (and topographically highest) sandstone bed in the Clarens Formation (Fig. 14D). In addition, sandstones associated with the upper contact frequently show ripple cross-lamination (Sr – Fig. 15D), horizontal stratification (Sh – Fig. 15D), low-angle cross-bedding (Sl) and less often, plant impressions (Fig. 15E), charred plant fragments and in situ and ex-situ petrified wood fragments (Fig. 15B).

4.2.1.2. Interpretation. The ropey surface texture preserved atop sandstones along the contact with the overlying basalts reflects the emplacement of low-viscosity pahoehoe lava flows over, soft, unlithified sandstones (also see Bordy et al., 2020, their Fig. 5A, B). In addition,

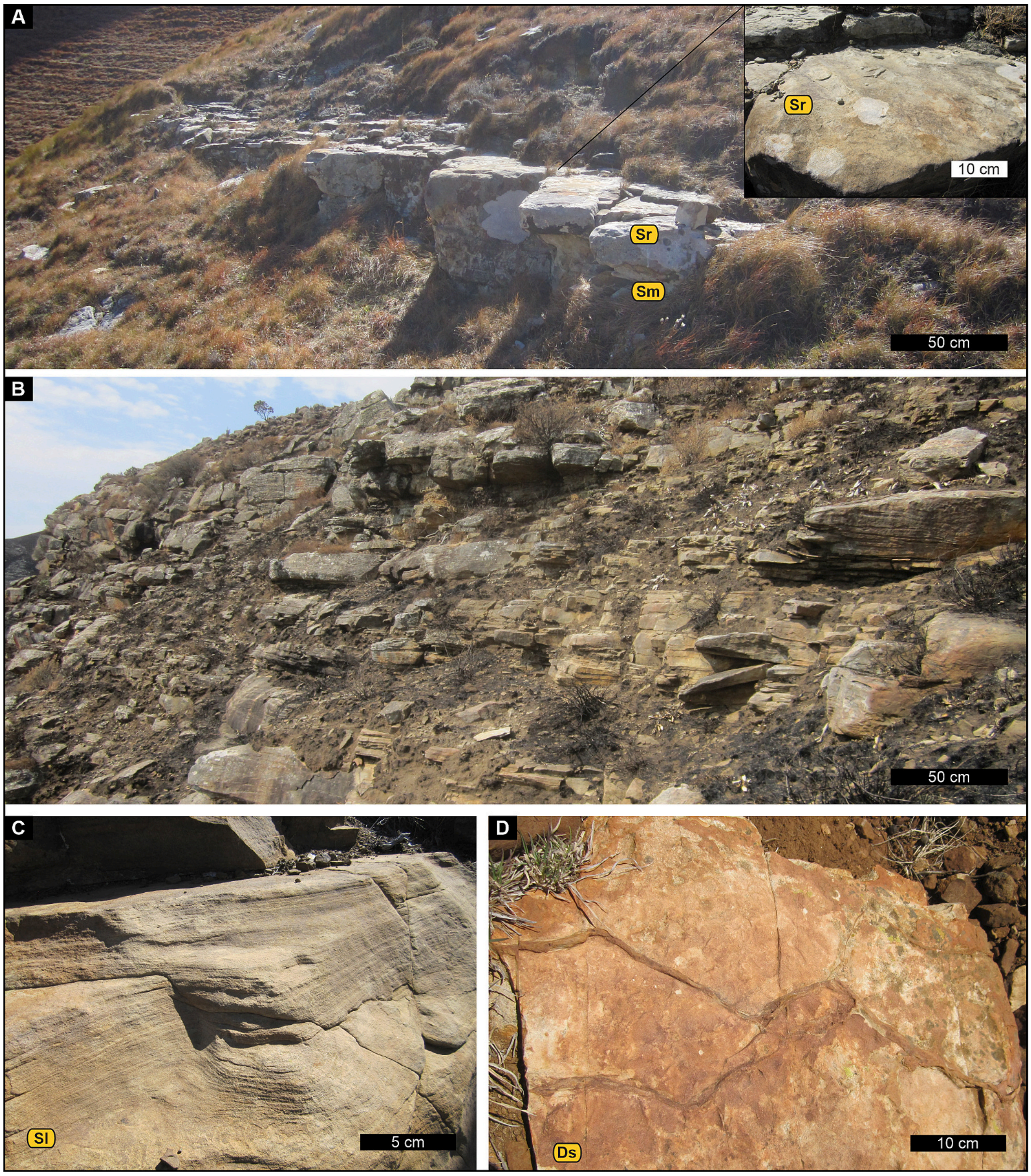

Fig. 11. Facies Association 5. **A.** Laterally extensive tabular massive sandstone with ripple cross-lamination and ripple marks (inset) on the upper surface at Ramatsediso's Nek. **B.** Stacked, thinly bedded, laterally extensive, horizontally stratified sandstones at Kamberg. **C.** Low-angle cross-bedding at Likosheng close to the upper contact. **D.** Desiccation cracks on a bedding plane surface in the uppermost part of the succession at Likosheng. See Table 1 for facies descriptions and Fig. 2 for site locations.

striations atop the youngest Clarens Formation sandstones could indicate that locally the lava flowed in a W-E direction (Jerram et al., 1999; Jerram and Stollhofen, 2002; Petry et al., 2007). The undulating upper contact of the Clarens Formation suggests that the lava poured out onto a dune field where dunes appear to have temporarily dammed the lava flow, which was also discussed by Beukes (1969, 1970) as well as Bordy et al. (2021). The onlapping sandstone interbed onto the youngest sandstone of the Clarens Formation, along with the appearance of wind ripples, indicates that the aeolian system was still active while the lava inundated the dune field. Moreover, the preservation of the wind ripple structures on the contact suggests that the lava flow passively blanketed the landscape (Jerram and Stollhofen, 2002). The combination of horizontally stratified (Sh) and ripple cross-laminated (Sr) sandstones are typical of unconfined fluvial flow (Hampton and Horton, 2007) and suggests that the facies association, in close proximity or in contact with the basalt, was deposited in relatively wet conditions, possibly in ephemeral unchannelised flow. This wetter phase in the terminal depositional period of the Clarens Formation is further strengthened by the presence of plant impressions, petrified wood fragments and in situ tree trunks (Bordy et al., 2021).

4.3. Facies association distribution and proportions

The facies association distribution and proportions of the Clarens Formation show that Facies Association 2 (Massive) dominates the upper and the lower succession (Fig. 16A, C) with Facies Association 1 (Aeolian dune) being subordinate. Facies Association 6 (Pluvial) is more prevalent in the lower succession, whereas in the upper part of the Clarens Formation, and Facies Association 6 are in higher abundance. In the middle section (Fig. 16B), Facies Association 1 dominates. Facies Association 3 (sand sheets) and Facies Association 4 (ephemeral channel) are present throughout the succession, although the former is the

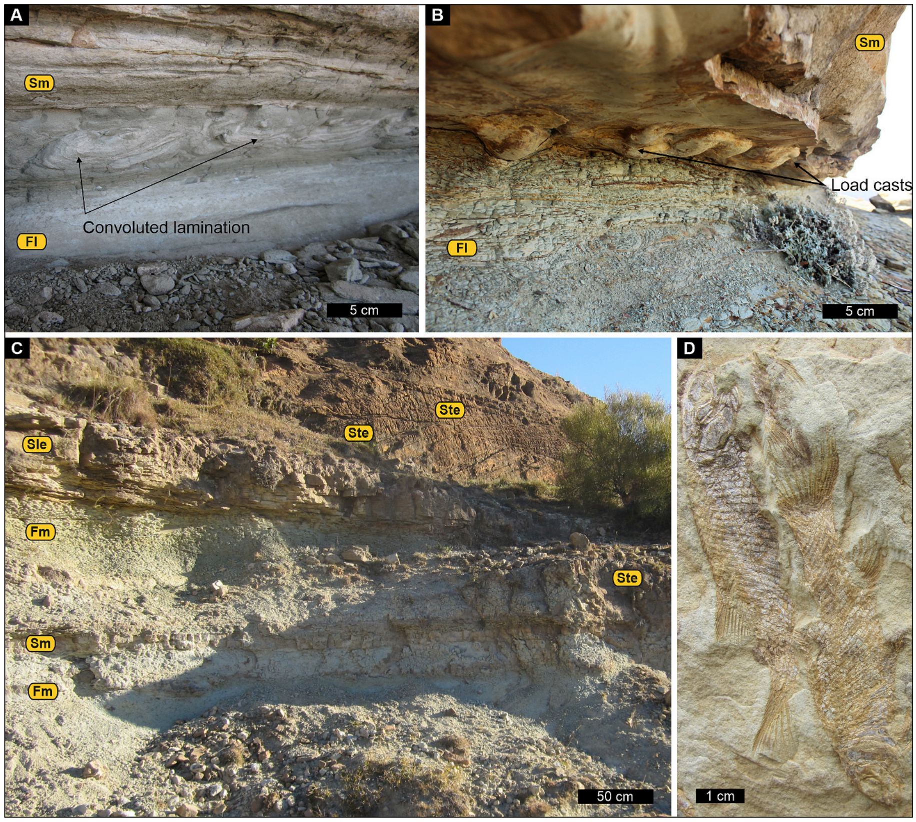

Fig. 12. Facies Association 6. **A.** Laminated mudstone with convolute bedding at Leeuwkop. **B.** Laminated mudstones with overlying load casts at Ramastediso's Nek. **C.** Lenticular massive mudstone interbedded with low-angle and large-scale cross-bedded sandstone layers at Koro-Koro. **D.** *Semionotus capensis* associated with the Facies Association 6 here seen in a sandstone building block on the farm Rietfontein close to Clarens, Free State, South Africa. See Table 1 for facies descriptions and Fig. 2 for site locations.

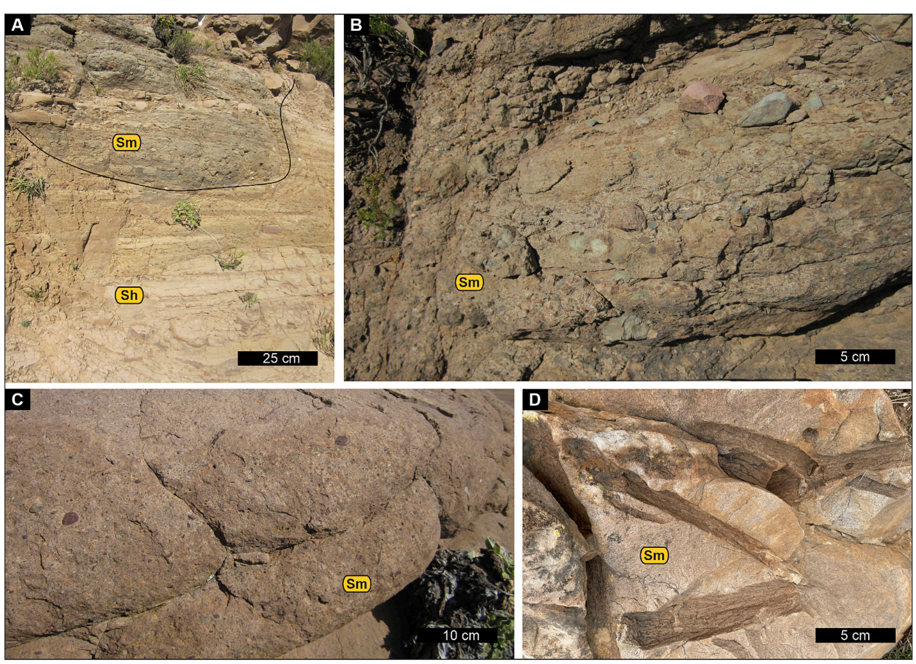

Fig. 13. Facies Association 7. **A.** Lenticular Debris Flow deposits amongst Facies Association 5 at the Talon section. **B.** Close up of Facies Association 7 from A. **C.** Massive sandstone with isolated clasts from Talon section. **D.** Wood impressions in a massive sandstone associated with Facies Association 7 at the Methinyeng study site. See Table 1 for facies descriptions and Fig. 2 for site locations.

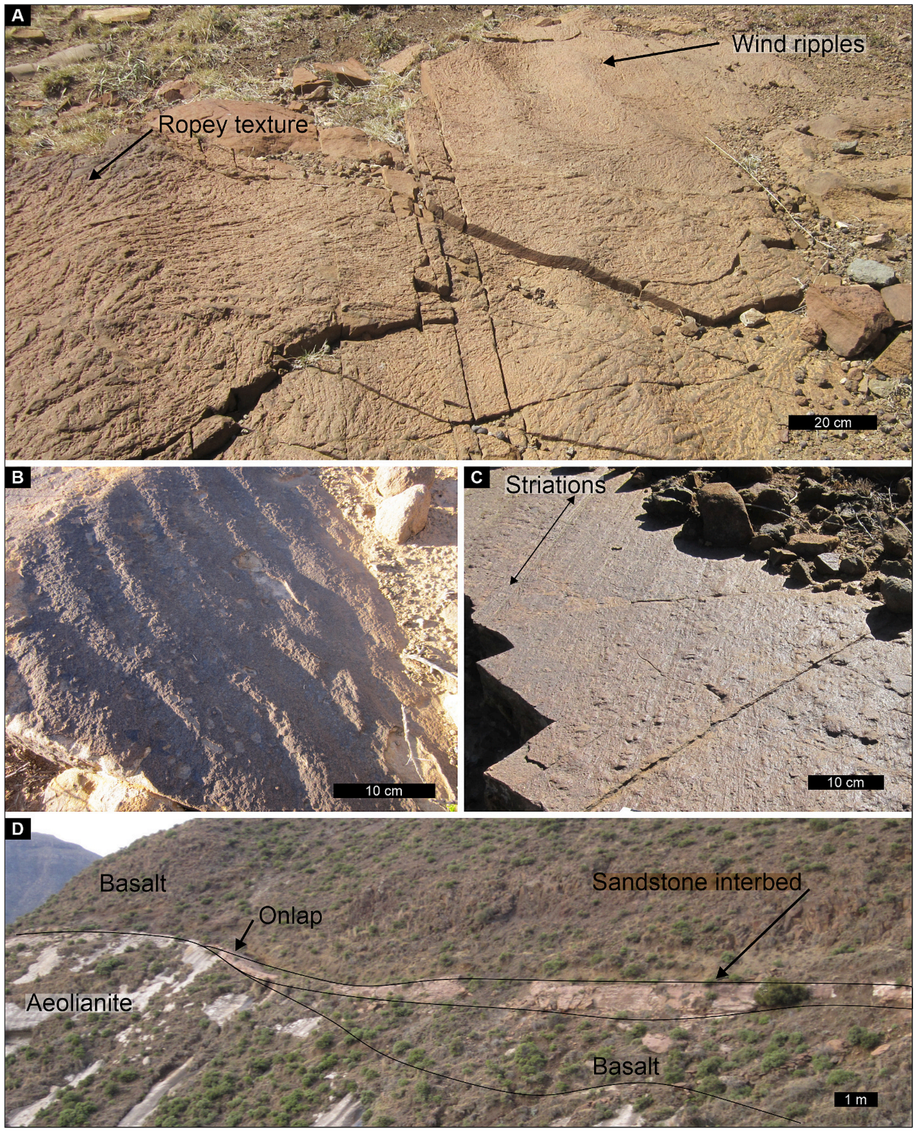

Fig. 14. Field features along the upper contact of the Clarens Formation. **A**. Wind ripples and ropey texture on the upper bedding plane of sandstones at Methinyeng. **B**. Ripple marks at Hellspoort. **C**. W-E oriented striations on the upper bedding plane of sandstones directly overlain by basalts. **D**. Onlapping relationship between a massive, uppermost Clarens Formation sandstone and a sandstone interbed within the overlying basalts of the lower Drakensberg Group (Barkly East Formation) at Mount Moorosi. For site locations, see Fig. 2.

least abundant in the upper part of the Clarens Formation (Fig. 16 C), whereas the latter is most abundant in the lower section. Overall, Facies Association 2 is the most dominant within the Clarens Formation (Fig. 16D), followed by Facies Association 1. The rarely observed Facies Association 7 (Debris flow) is the least abundant (< 1 %) and confined to zones 1 and 3 only (Fig. 16).

The vertical variations in these facies associations discussed above (Fig. 16) supports the zonation proposed by Beukes (1969, 1970), and for the purposes of the discussion, will be referred to as zone 1 to 3. Zone 1 comprises dominantly Facies Association 2 (massive) co-occurring with the appearance of Facies Association 6 (pluvial). Zone 2 is characterized by the dominance of Facies Association 1 (Large-scale cross-bedded), whereas Zone 3 is defined by the reappearance of dominantly Facies Association 2 (massive) and the co-occurrence of Facies Association 4 (fluvial channlised) and 5 (fluvial unchannelised). Notably, Facies Association 3 (sand sheets) and Facies Association 7 (debris flow) are present in all zones to different degrees.

4.4. Formation thickness and palaeocurrents

The input data for the thickness estimation of the Clarens Formation includes 33 data points observed during this study and 94 thickness data points extracted from Du Toit (1904, 1905), Stockley (1947), Beukes (1969), Robinson et al. (1969) and Eriksson (1983), which are all outcrop measurements from sedimentary logs and detailed, field-mapping exercises. The measurements of Stockley (1947) are based on the principles outlined by Van Eeden (1937), where the transitional succession with the underlying Elliot Formation is included into the Clarens Formation thickness data, and for this reason may reflect slightly different thicknesses than those reported in other studies. These combined results show that a range of 90 to 150 m represents a good average thickness for the Clarens Formation (Fig. 16), and that the maximum thickness value of the unit is 300 m (Fig. 16C). As already pointed out by Beukes (1969), the Clarens Formation reaches its thickest part in the Eastern Cape and southern Lesotho along a trough axis running northeast to southwest (Fig. 16A). Despite the localised thickness fluctuations (e.g., 0 m near Qachas Nek, Elliot and Maclear in the

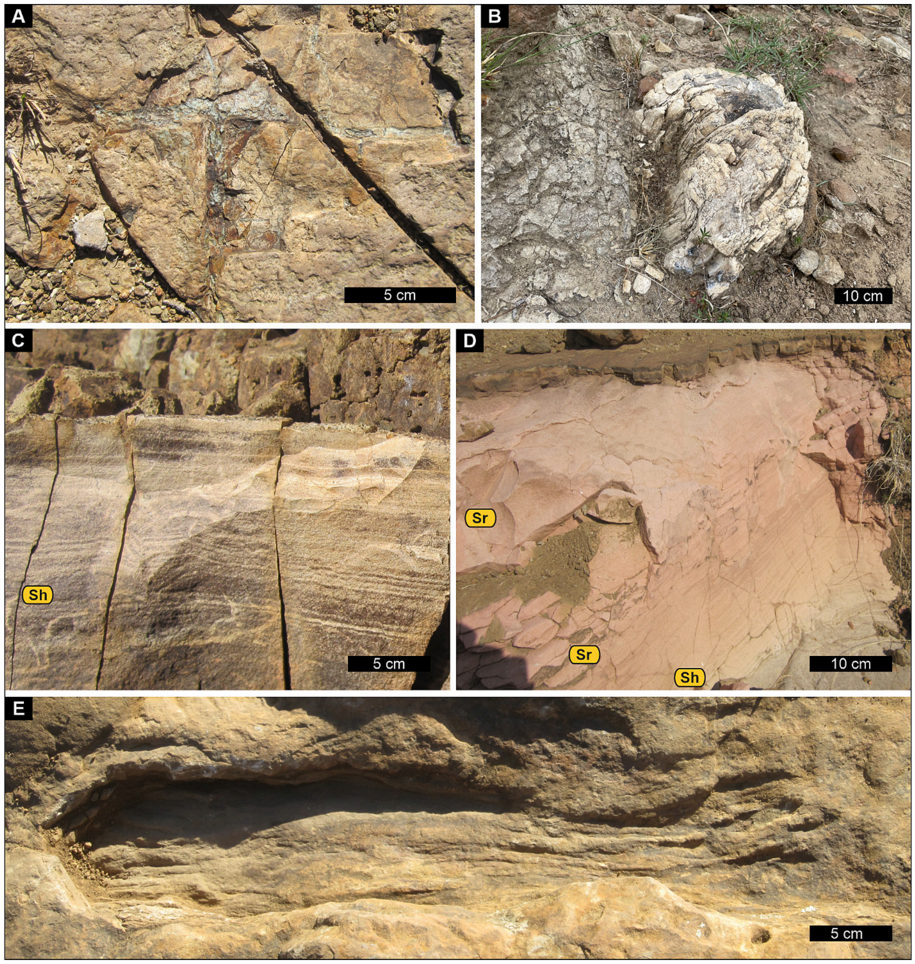

Fig. 15. Field features along and near the upper contact of the Clarens Formation. **A.** Desiccation cracks on the upper contact at Leeuwkop. **B.** In-situ tree trunk found on the contact at Methinyeng. **C.** Horizontally stratified sandstone below the upper contact. **D.** Ripple cross-laminated sandstone below the upper contact at Methinyeng. **E.** Plant impression in massive sandstone ~1 m below the upper contact. See Table 1 for facies descriptions and Fig. 2 for site locations.

Eastern Cape of South Africa - Fig. 156, C), a subtle regional south to north decrease in thickness is apparent given that the 200 m contours are only traceable in the southern outcrop area. In addition, the thickness distribution is more consistent in the northern outcrop area. Palaeowind directions measured from the foreset dip-directions of large-scale cross-bedded sandstones (mostly associated with the Facies Association 1) record a flow direction from roughly west to east with a high consistency ratio (Fig. 17B), although a localised deviation from the overall trend is observed in the basal large-scale cross-bedded sandstones at Balloch.

5. Discussion

5.1. Depositional model

The distribution of facies associations in the Clarens Formation suggests that various large-scale drivers were at work during the deposition of this largely aeolian system. The erg was relatively dynamic with expansions and contractions throughout the depositional period (Fig. 15). These fluctuations were concomitant with dramatic lateral facies shifts that can be attributed to changes within a typical zoned ergs, where variations in facies are a result of spatial fluctuations in the erg (dry inner erg to wet erg margin/outer erg conditions - Langford and Chan, 1989; Kocurek and Havholm, 1993; Mountney and Jagger, 2002; Mountney, 2006; Mayoral et al., 2021). Moreover, the vertical facies changes (i.e., tripartite zonation of the formation) reflect erg margin shifts related to a temporal wet-dry-wet climate megacycle as first identified by Beukes (1969, 1970) and recently refined by Bordy et al. (2021) for the middle to upper Clarens Formation in southern-central Lesotho.

5.1.1. Zone 1: establishment of aeolian conditions

The facies distribution for the oldest zone in the Clarens Formation indicates relatively small and isolated dune fields with associated aeolian sand sheets preserved along the erg margins. The development of sand sheets has been linked to conditions that limit the development of aeolian dunes such as diminishing sand supply and flooding and/or water-table rise (Kocurek and Nielson, 1986; Langford and Chan, 1993; Mountney, 2006). Sand sheets have also been shown to be prevalent along the fore erg and often appear associated with transitional environments where fluvial and aeolian processes interact (Porter, 1986; Mountney, 2006; Al-Masrahy and Mountney, 2015). Facies associations on the eastern margin suggests the presence of ephemeral channel deposits that were highly cannibalistic, reworking older in-channel and/or overbank deposits. Moreover, pluvial deposits appearing in close proximity to Facies Association 1 is indicative of wet interdune conditions.

Deposition of loess may be favoured during a transition to more humid conditions (Pye, 1995), although this brings into question what is meant by humid conditions. In the case of loess, its appearance has been shown to reflect accumulation linked to semi-arid conditions or sub-humid conditions (Porter and Zhisheng, 1995; Muhs and Bettis, 2003; Fitzsimmons et al., 2013) where episodic moisture promotes the growth

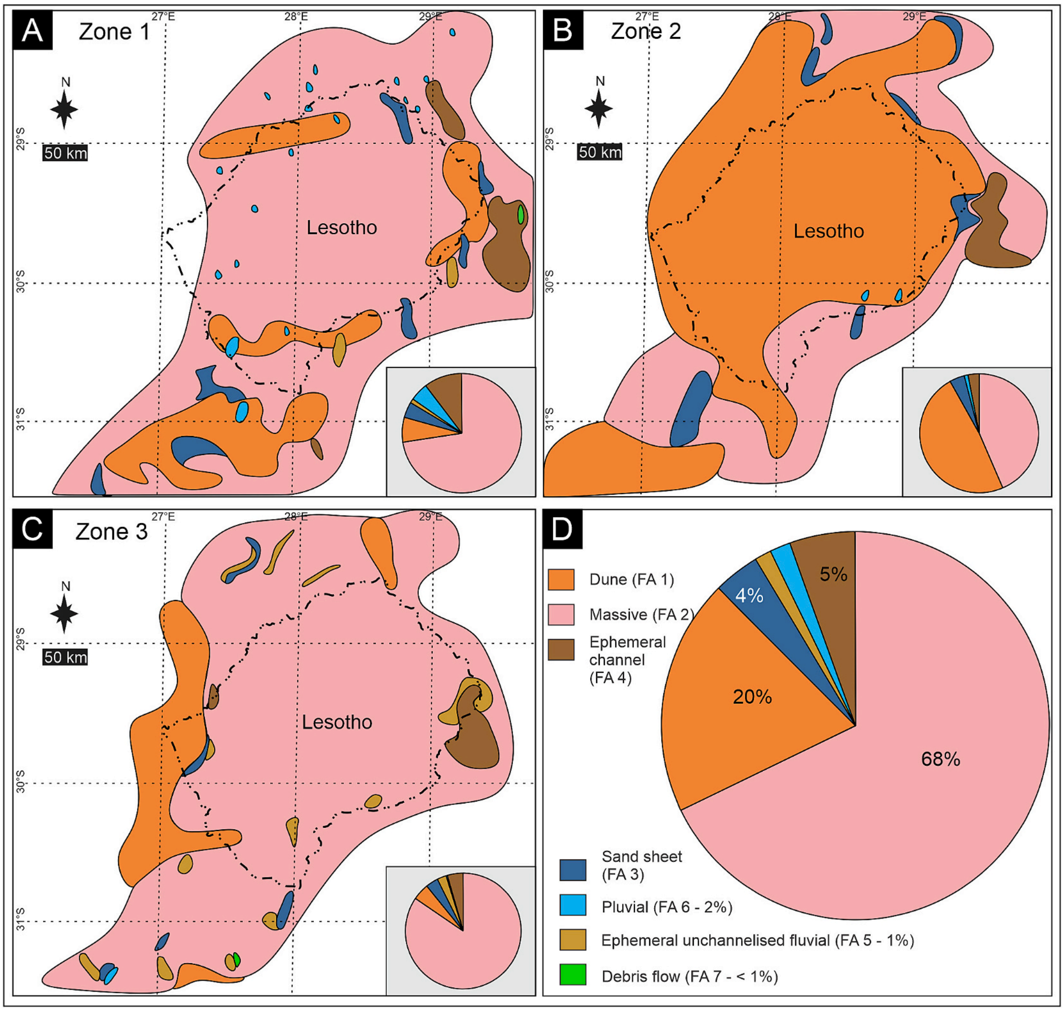

Fig. 16. Facies association distribution and proportions of the Clarens Formation. **A**. Zone 1. **B**. Zone 2. **C**. Zone 3. **D**. Overall facies association proportions of the Clarens Formation.

of vegetation or moist surfaces to capture the sediments. The appearance of loess is therefore suggestive of cool, dry conditions which is climatically distinct from the hyper aridity associated with large scale erg development (migrating dunes). Given this, the massive sandstones downwind from the interpreted erg deposits also suggest the presence of sandy loess to loess deposits, which in turn indicate the prevalence of dust storms. This upwind erg is interpreted from both the localised appearance (western part of the basin) of Facies Association 1 within zone 1, and the regional distribution of Clarens Formation equivalents throughout southern Africa (Fig. 2). Overall, the isolated nature of migrating aeolian dune deposits, which appear with relatively scarce pluvial deposits (i.e., interdune deposits), reflects a wet-to-dry aeolian system, while the co-occurrence of massive and aeolian sand sheet deposits suggest that this part of the Clarens Formation was dominated by erg margin processes during a semi-arid (episodically wet) period. Massive deposits can also be linked to dune slumping related to high precipitation and water infiltration as documented in modern and ancient aeolian settings (Loope et al., 1998; Sweeney and Loope, 2001; Simpson et al., 2002; Heness et al., 2014), which also supports a more humid climate interpretation for Zone 1.

5.1.2. Zone 2: expansion of the erg

The facies association distribution in Zone 2 of the Clarens Formation shows a notable increase in aeolian dune deposits (Fig. 15B) along with massive and aeolian sand sheet deposits. This increase in Facies Association 1, and the corresponding decrease in Facies Association 2 suggests that there was an increase in aridity, which allowed for an increase in sand availability and ultimately expansion of the erg to the east (downwind). Similar erg expansion in the Permian Organ Rock Formation in the USA was linked to climatic aridification (Cain and Mountney, 2009). In addition, the general lack of interdunal facies preservation suggests that this part of the Clarens Formation was deposited under dry aeolian conditions (Kocurek and Havholm, 1993;, Mountney, 2006), while localised lacustrine and fluvial deposits (Facies Association 4, 5 and 6) can be ascribed to the incursion of fluvio-lacustrine systems along the southern and eastern outcrop areas.

5.1.3. Zone 3: shrinkage of the erg

Facies associations within Zone 3 (Fig. 15C) indicate the dominance of massive deposits with subordinate aeolian dune and aeolian sand sheet deposits. The prevalence of massive deposits suggests that dust storms were once again active. Similar to Zone 1, the presence of massive sandstones interpreted as aeolian dust deposits can imply a change from hyper aridity to more semi-arid conditions indictive of increased moisture that enhances dust deposition (Porter and Zhisheng, 1995; Muhs and Bettis, 2003; Fitzsimmons et al., 2013). Spatially, aeolian sand sheet deposits appear in close proximity to the migrating aeolian dune deposits which is limited to the western outcrop area, while Facies Association 5 appear sporadically to the east of these. Overall, this may be indicative of an increase in surface moisture that limited wind-blown sediment availability resulting in erg margin retreat and shrinking of the erg to the west (upwind). This allowed for the

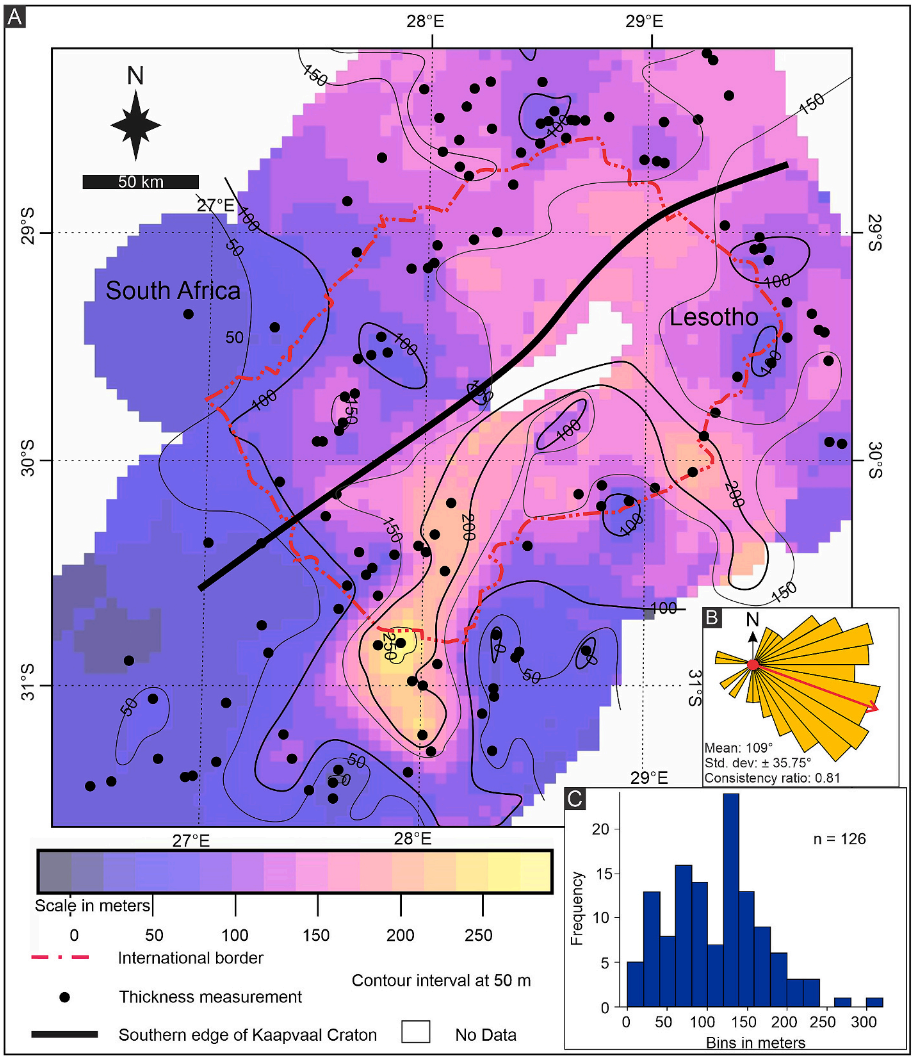

Fig. 17. Isopach and palaeocurrent data of the Clarens Formation in the MKB. **A.** Thickness map with 50 m interval contour lines. Note the highest thickness zone in southern and central Lesotho. **B.** Palaeocurrent rose of measured flow directions in the Facies Association 1. **C.** Histogram of thickness data points showing a range from 0 to >300 m. 5. (For interpretation of the references to colour in this figure legend, the reader is referred to the web version of this article.)

incursion of fluvio-lacustrine processes into the dune field, resulting in episodic wet aeolian conditions. Limited occurrence of debris flow processes (with basaltic material incorporated into it) and basalts amongst migrating aeolian dunes in the uppermost Clarens Formation suggests that the aeolian system was still active during a wet period in the Late Pliensbachian during the outpouring of the earliest Karoo lava flows (Duncan et al., 1997; Moulin et al., 2011, 2017; Svensen et al., 2012). Moreover, the occurrence of terminal shallow lakes associated with lava deltas in the Clarens Formation during a Late Pliensbachian humid phase and before large-scale extrusion of the Karoo lava flows was discussed in Bordy et al. (2021).

5.2. Synthesis of the erg development

Interpretation of the Clarens Formation as a vast sand sea succession date back to some 100 years ago to Du Toit (1918 p.36). The formation of these desert conditions in the MKB during the Early Jurassic was suggested to be the cause of the latitudinal position of the MKB along with the orographic effect of the Cape Fold Belt that would have created a rain-shadow effect. This further exacerbated the continental interior position of the MKB (Loope et al., 2004; Bordy, 2008; Bordy and Head, 2018). As reviewed in Bordy and Head (2018), Beukes (1969, 1970) recorded the three stratigraphic zones in the Clarens Formation that reflect a temporal wet-dry-wet megacycle across the basin, whereas Eriksson (1981, 1986) identified spatial domains in the Clarens Formation in the KwaZulu-Natal Drakensberg region.

This synthesis shows that both spatial and temporal controls were active during the deposition of the Clarens Formation. The lateral facies changes illustrate a transition from dry erg interior to wet erg margin typical of spatial variation in wetness conditions in a large erg system (Mountney and Thompson, 2002; Mountney and Jagger, 2004), whereas the vertical facies changes illustrate dramatic erg margin shifts related to temporal climate megacycles (Figs. 14, 16). This implies that during semi-arid (increased moisture) conditions, the erg was smaller and episodic wet phases allowed for the incursion of more fluvial and lacustrine systems into the dune field while aeolian dust deposition (loess) dominated downwind along the outer erg situated to the east of the basin. During arid conditions as suggested by the dominance of Facies Association 1, hyper arid climatic conditions set in, increasing sediment availability which resulted in erg growth at the expense of the dust plains, while also pushing fluvial and lacustrine processes further east. During the initial stages of Karoo lava extrusion, the aeolian system and related marginal lacustro-fluvial processes were still active. Given this field-based evidence associated with the upper contact, a conformable relationship is confirmed for the contact between the Clarens Formation and the overlying Drakensberg Group (also see Bordy et al., 2021).

5.3. Comparison with ancient fluvial-aeolian deposits

The distribution of the facies associations combined with the facies proportions per zone (Fig. 16), indicates that large-scale, spatiotemporal changes occurred in the depositional environment. These may be related to spatial and temporal fluctuations in sediment supply and availability, combined with atmospheric circulation patterns and climate fluctuations (Kocurek and Havholm, 1993; Mountney and Thompson, 2002; Mountney and Jagger, 2004; Mountney, 2006). These facies can broadly be attributed to deposition along an erg margin and identified based on various features and criteria. These criteria are: 1) differences in grain size and sorting that would represent downwind changes; 2) changes in the complexity of dune-size and stratification; 3) changes in dune spacing; 4) an increase in sand sheet abundance; 5) the prevalence of bioturbation and; 6) an increase in facies associated with non-aeolian deposition (Langford and Chan, 1993). When considering these, an increase in non-aeolian deposits, a downwind grain size decrease as well as increased aeolian sand sheet- and massive deposits suggests that deposition of the Clarens Formation occurred along an erg margin to outer erg.

Such erg dynamics are well documented from various ancient aeolianites (e.g., Candeleros Formation of Argentina – Pérez Mayoral et al., 2021; the Cedar Mesa Sandstone in the USA – Langford and Chan, 1993; Mountney and Jagger, 2004; Gahlo du Miguel Formation in Brazil – Basilici et al., 2021), where damp and wet interdunes progressively increased towards the erg-margin, a classical feature of the zoned erg deposition model (Mountney and Jagger, 2004; Mountney, 2006). In addition, the level of the water table, along with its temporal fluxes, also play an important role in the complexity of the aeolian facies (Mountney and Thompson, 2002; Mountney and Jagger, 2004; Mountney, 2006), and therefore interdunes expand and contract in response to relative water-table fluctuations which results in several stacking pattern expressions based on how these parameters interacted.

A typical erg margin deposit has been described by Mountney and Jagger (2004) for the Permian Cedar Mesa Sandstone, and similarly, in the Mesoproterozoic Galho do Miguel Formation of SE Brazil. For the Cedar Mesa Sandstone, Mountney and Jagger (2004) observed temporal fluctuations in bedform size and angle of climb combined with episodic changes in the relative water table. In the case of the Candeleros Formation, facies have been interpreted by Pérez Mayoral et al. (2021) as a typical erg margin deposit where stratigraphic changes in the facies associations can be attributed to the expansion and contraction of the erg. In essence, episodes of erg contractions were related to a rise in water-table, whereas erg expansions reflected a fall in water table (Pérez Mayoral et al., 2021). Similarly, the Clarens Formation reflects expansions and contractions of the erg when a water table fall allowed for the increased availability of sediments for entrainment.

During semi-arid phases, moisture restricted the availability of sediment, and in turn, affected sediment availability for the construction of dune bedforms (Crabaugh and Kocurek, 1993; Neuman and Scott, 1998; Al-Masrahy and Mountney, 2015). This type of fluvial interaction is described by Al-Masrahy and Mountney (2015) as one influenced by a raised water table and can be classified based on the appearance of characteristic wet and damp aeolian features such as adhesion structures, wavy lamination, aqueous ripple marks, brecciated laminae, and contorted structures. Such features have been identified for the lower Clarens Formation (Head and Bordy, 2023a), supporting the occurrence of a raised water table for Zone 1. These phases of raised water tables are well known to stimulate accumulation and preservation in aeolian systems, particularly where it is linked to a subsiding basin (Mountney and Thompson, 2002; Al-Masrahy and Mountney, 2015; Cosgrove et al., 2022), such as that of the tectonic setting of the Clarens Formation in the subsiding foresag of the Karoo Foreland system (Bordy et al., 2004b, 2005).

Loess deposits with close dune sources often preserve interbedded sandstones from both dust and dune facies (Pye, 1995; Al-Masrahy and Mountney, 2015) and this type of interfingering relationship has been documented on the Chinese Loess Plateau, where large-scale, cross-bedded sand has been observed within loess deposits. Based on optically stimulated luminescence dating, the dunes were interpreted to have formed in a period of amplified aridity (Long et al., 2012). These results can be used to infer a strong climatic control on the abundance of migrating dunes and suggests a similar case for the abundance of migrating aeolian dune deposits identified in zone 2 of the Clarens Formation. Additionally, the provenance of the Clarens Formation indicates similar zircon crystal dates for both dune facies and loess facies (Head et al., 2024), suggesting that the sediments were derived from the same source terrains, and in turn, dust particles were likely produced in the erg.

Episodic fluvial incursions may be prevalent along fluvially dominated erg margins, and several types of fluvial interactions can be identified in modern erg margin settings (Mountney and Jagger, 2004; Mountney, 2006; Al-Masrahy and Mountney, 2015). The preservation of ephemeral channel deposits and ephemeral unconfined fluvial deposits on the eastern erg margin of the Clarens Formation reflects differing degrees of fluvial erg infiltration throughout the succession. This type of fluvial-aeolian interaction is described by Al-Masrahy and Mountney (2015) as fluvial infiltrations linked to multiple sheetflood sources. Fluvial systems of this type are expressed as unconfined deposition along a relatively low-gradient plain being particularly active after rainstorm events (Al-Masrahy and Mountney, 2015; Priddy and Clarke, 2020). Such unconfined flow can also be explained by the effect of rainstorms on the desert landscape, where limited infiltration of water into the subsurface is offset by high precipitation volumes resulting in overland flow (Goudie, 2013). This feature may explain the wide geographic distribution of ephemeral unconfined fluvial deposits in the Clarens Formation, especially for the upper Clarens Formation (Zone 3).

Overall, the current reassessment of the distribution of facies associations confirms both the validity of the tripartite zonation of the Clarens Formation as defined by Beukes (1969, 1970) and the interpretation of a wet-dry-wet climate megacycle during deposition. Similar climatic megacycles have been observed in other ancient aeolian systems associated with fluvio-lacustrine processes and attest to the common interaction of wet-to-dry aeolian processes in the Clarens Formation.

5.4. Early Jurassic climate in southwestern Gondwana

Globally, the Early Jurassic is characterized by extreme environmental variations, when the dominant warm conditions were interrupted by episodic cool phases (Price, 1999; Baghli et al., 2020). The arid climate during the Early Jurassic of southwestern Gondwana has been attributed to the continentality of the MKB combined with the orographic effect of the Cape Fold Belt during the Late Triassic to Early Jurassic (Veevers, 2004; Bordy, 2008; Bordy and Head, 2018), a trend that has been associated with many Jurassic deposits of southwestern Gondwana (Holzförster et al., 1999; Jerram et al., 1999, 2000; Loope et al., 2001: Fig. 1; Bordy and Catuneanu, 2002; Scherer and Lavina, 2005; Scherer and Goldberg, 2010; do Amarante et al., 2019). The Clarens Formation also shows prominent vertical facies changes that suggests a more complex wet-dry-wet climatic megacycle during deposition (Fig. 17). In addition to the classical work of Beukes (1969, 1970) and Eriksson (1979, 1981, 1986), Rampersadh et al. (2018) and Bordy et al. (2021) have also described field evidence for the semi-arid (episodically wet) periods associated with the lower and uppermost Clarens Formation, respectively.

Despite the evidence that northern Gondwana (south Tethys Sea) was a more arid relative to the north-western Tethys (Aberhan, 2001; Van de Schootbrugge et al., 2005), Baghli et al. (2020) has shown that the climatic trend for northern Gondwana is very similar to that of

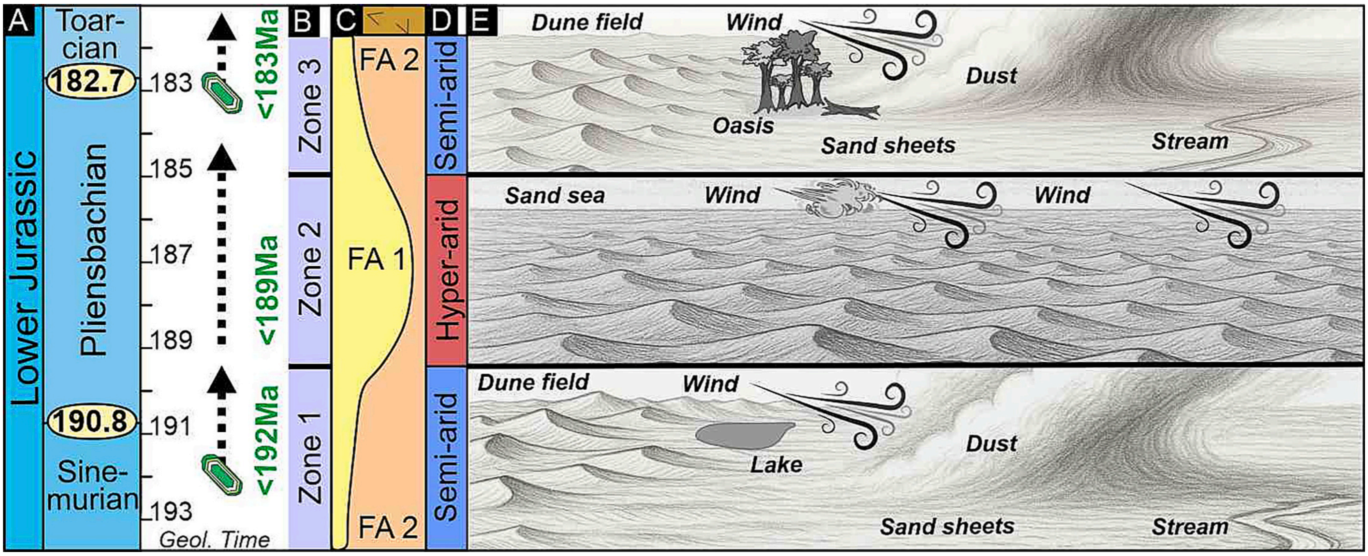

Fig. 18. Stratigraphy of the Clarens Formation. **A.** Maximum Depositional Ages (MDA) for the Clarens Formation from Head et al. (2024). Note that the middle part of the succession lacks a clearly defined MDA due to overlapping uncertainties; however, zircon dates indicate a cluster around ~189. **B.** Zonal interpretations based on vertical facies distribution. **C.** Stratigraphic variation in dominant facies associations—see Tables 1 and 2 for facies descriptions. The Drakensberg Group (brown) marks the large-scale extrusion of Karoo continental flood basalt ~183 Ma ago. **D.** Stratigraphic variation in climatic phases. **E.** Palaeogeographic evolution of the Clarens Formation during the Early Jurassic, indicating dominant wind direction from the west. (For interpretation of the references to colour in this figure legend, the reader is referred to the web version of this article.)

Boreal and Tethyan sections (Hesselbo et al., 2000; McArthur et al., 2000; Jenkyns et al., 2002; Bailey et al., 2003; Rosales et al., 2004; Van de Schootbrugge et al., 2005; Gómez et al., 2008; Suan et al., 2008; Dera et al., 2011; Armendáriz et al., 2012; Korte and Hesselbo, 2011; Korte et al., 2015; Li et al., 2012; Harazim et al., 2013) with the exception of negative oxygen and carbon isotope excursions close to the lower and upper boundaries of the Pliensbachian.

The field-based evidence from this study combined with absolute age dates (Fig. 18, Head et al., 2024) and the suggested global climatic trend recorded in the Tethyan region indicates a late Sinemurian cooling, an early Pliensbachian warming followed by an early late Pliensbachian cooling phase (Dera et al., 2011; Gómez et al., 2016; Alberti et al., 2019; Baghli et al., 2020; Bordy et al., 2020, 2021). Given the facies associations within the Clarens Formation, the general climate in southwestern Gondwana can be envisioned as semi-arid to arid having a dry aeolian system with episodic phases of wet aeolian activity, while consistent and continuous windy and dusty conditions prevailed along the outer erg to erg margin. Ephemeral lakes and rivers were active along the erg margin, and during semi-arid phases, precipitation may have resulted in a relative rise of the water table.

Global atmospheric circulation patterns of Chandler et al. (1992), as discussed by Loope et al. (2004) – see their Fig. 5), suggests that seasonal wind reversal occurred in both hemispheres during the Early Jurassic of Pangaea and is consistent with the measured SE- directed wind regime interpreted for the Clarens Formation, given the palaeolatitue of the basin (Sciscio et al., 2017). This has also been identified in Jurassic aeolianites in the USA and Brazil that show a strong seasonality associated with a monsoonal palaeo-climate (Parrish and Peterson, 1988; Chandler et al., 1992; Loope et al., 2004; Scherer and Goldberg, 2010). These reversals were reported to cause strong dune migrating north-westerlies and weaker southerly winds for the Navajo Sandstone, resulting in a consistent north-westerly trend in the palaeo-flow directions, while wet to damp aeolian conditions have also been suggested to come about linked to monsoonal climate for the Sherwood Sandstone Group in the UK (Cosgrove et al., 2025).

Although monsoonal seasonality has not been observed in the Clarens Formation, foresets in large-scale, cross-bedded sandstones being composed of grain flow and translatent ripple cross-lamination can indicate a strong seasonality in wind patterns (Kocurek, 1991). In a similar way, the consistent south-east directed foresets within Facies Association 1 of the Clarens Formation may be related to such mid-latitude westerlies associated with atmospheric circulation linked to large-scale Hadley flow, which is believed to have been active since the Palaeozoic (Scotese et al., 1999; Cosgrove et al., 2021a). During the summer months, seasonal reversals came about as a result of the movement of the intertropical convergence zone (ITCZ) and caused weaker south-westerly winds that may have led to the deposition of the translatent ripple stratification. Despite various Pangaea atmospheric circulation models (Kutzbach and Gallimore, 1989; Kutzbach, 1994), the consistent south-easterly oriented cross-bed foreset measurements reported from the Clarens Formation (Fig. 18) supports the Early Jurassic circulation model of Chandler et al. (1992).

5.5. Thickness trends of the Clarens Formation in the Karoo foreland basin context

The current thickness estimation map (Fig. 15A) confirms the previously identified northeast-southwest directed trough (Beukes, 1969, 1970; Robinson et al., 1969; Johnson, 1976; Eriksson, 1981, 1986) as well as the extreme but localised thickness fluctuations in the southern outcrop area. Sites where the Clarens Formation is absent have been ascribed to early onset lava extrusion, or alternatively, localised erosion due to authigenic processes (e.g., scouring by rivers) or non-deposition (aeolian by-pass) of the sediments due to varied dune distribution across paleo-topographic heights (e.g., Du Toit, 1905, 1910; Du Toit, 1918; Beukes, 1969, 1970; Robinson et al., 1969).

The northeast–southwest oriented thickness trough in the Clarens Formation isopach map aligns well with the orientation of the southern edge of the Kaapvaal Craton (Fig. 15; Schmitz and Rooyani, 1987, Skinner et al., 1992; Bordy et al., 2004b, Bordy et al., 2005). Therefore, the subtle regional decrease in thickness in the Clarens Formation could be related to rheological (e.g., viscoelastic) variations in the Karoo basement, where the depositional area that is underlain by the Namaqua Natal Mobile Belt was more prone to subsidence compared to the regions underlain by the more rigid Kaapvaal Craton (Schmitz and Rooyani, 1987; Bordy et al., 2005). Similar thickness trends related to the basement rheology as well as to the position of the southern edge of the Kaapvaal Craton have been observed in the pre-Clarens Formation depositional history of the MKB (e.g., Molteno Formation – Hancox, 1998; Elliot Formation – Bordy et al., 2004b, 2005).

Given that there are no significant facies changes seen for the Clarens Formation in terms of this boundary, thickness differences in the pluvial deposits of the Clarens Formation (see Head and Bordy, 2023a) that are attributed to both climatic factors and differential subsidence, may be related to the aforementioned variation in basement rheology. Additionally, the thickness trend in the Clarens Formation, being consistent with thickness trends for the Elliot Formation, supports the terminal foresag basin model for the upper Stromberg Group (e.g., Bordy et al., 2004b, 2005). Notably, *syn*-sedimentary normal faulting in the Clarens Formation at Moyeni (Haupt, 2018) and Siberia (Bordy et al., 2004b) also suggests that, at least locally, extensional tectonics in the MKB may have started to be active from the Sinemurian onwards.

6. Conclusion

The sedimentary facies of the Clarens Formation reflect a depositional environment where eastward migrating dunes and down-wind aeolian dust were deposited along the erg margin to outer erg of an extensive aeolian system. Aeolian sand sheets formed transitional features along erg margins, while fluvial-lacustrine systems penetrated the inner erg from the east. Contemporaneous climatic trends reported from the Tethyan margin of Gondwana are closely mimicked by the wet-dry-wet (fluctuating between semi-arid to hyper-arid) megacycle identified in the Clarens Formation suggesting that this may have been of global significance in the Early Jurassic. This climatic megacycle is based on the vertical facies changes that initially reflect an episode of wet aeolian deposition, when limited sediment availability enhanced the deposition of aeolian dust on an extensive downwind loess plain. Following the wet phase, aridification of the environment resulted in increased aeolian sediment supply causing an expansion of the erg. The subsequent wet phase in the aeolian system ensued across most of the basin and was still active during the onset of early extrusion of the continental flood basalts associated with the Karoo-Ferrar Igneous Province. The thickness trends indicate a subtle north to south increase with extreme localised thickness fluctuations in the southern outcrop area, whereas the northern outcrop area shows a more constant thickness. This thickness trend may reflect the variation in the basement rheology and supports the foresag basin model during the terminal phase of the MKB evolution. As a whole, the Clarens Formation uniquely preserves evidence of erg dynamics associated with an ancient erg margin to outer erg setting throughout several climatic transitions during the early stages of Gondwana's fragmentation. As such, the rocks of the Clarens Formation can lend itself to broadening our understanding of past Earth system behaviour along with its implications for modern climate and ecosystem studies.

CRediT authorship contribution statement

Howard V. Head: Writing – review & editing, Writing – original draft, Visualization, Validation, Project administration, Methodology, Investigation, Formal analysis, Data curation. **Emese M. Bordy:** Writing – review & editing, Visualization, Validation, Supervision, Project administration, Funding acquisition, Formal analysis, Conceptualization.

Funding

This research was financially supported by grants to EB from the National Research Foundation (NRF South Africa) related to the Programme for Rated Researchers (CPRR) and the African Origins Programme (AOP; grant number 93544, 113394, 98825). Additional funding grants were also awarded to EB from GENUS (DST-NRF Centre of Excellence in Palaeosciences; grant number CoE Pal 2019, 2020). HH was awarded post graduate bursary support from GENUS (CoE Pal) and UCT's Vice Chancellor scholarship.

Declaration of competing interest

The authors declare that they have no known competing financial interests or personal relationships that could have appeared to influence the work reported in this paper.

Acknowledgements

We thank Miengah Abrahams, Akhil Rampersadh, Yambi Dinis, Riyaad Mukaddam and Lara Sciscio for field assistance during various field trip throughout 2018 to 2021. We are also grateful to the landowners and farmers who graciously granted access to their land, as well as Ezemvelo KZN wildlife for field support and access to the South African National Parks in KwaZulu Natal. We thank Howard Falcon-Lang for editorial handling, along with Judith Totman Parish, Edward Simpson and one anonymous reviewer for constructive feedback on the paper.

Data availability

The authors confirm that all data necessary for supporting the scientific findings of this paper have been provided.

References

Aberhan, M., 2001. Bivalve palaeobiogeography and the Hispanic Corridor: time of opening and effectiveness of a proto-Atlantic seaway. Palaeogeogr. Palaeoclimatol. Palaeoecol. 165 (3–4), 375–394. https://doi.org/10.1016/S0031-0182(00)00172-3.

Alberti, M., Arabas, A., Fürsich, F.T., Andersen, N., Ziółkowski, P., 2019. The Middle to Upper Jurassic stable isotope record of Madagascar: Linking temperature changes with plate tectonics during the break-up of Gondwana. Gondwana Res. 73, 1–15.

Allen, J.R.L., Banks, N.L., 1972. An interpretation and analysis of recumbent-folded deformed cross-bedding. Sedimentology 19 (3–4), 257–283. https://doi.org/10.1111/j.1365-3091.1972.tb00024.x.

Al-Masrahy, M.A., Mountney, N.P., 2015. A classification scheme for fluvial–aeolian system interaction in desert-margin settings. Aeolian Res. 17, 67–88. https://doi.org/10.1016/j.aeolia.2015.01.010.

do Amarante, F.B., Scherer, C.M., Aguilar, C.A.G., dos Reis, A.D., Mesa, V., Soto, M., 2019. Fluvial-eolian deposits of the Tacuarembó formation (Norte Basin–Uruguay): Depositional models and stratigraphic succession. J. S. Am. Earth Sci. 90, 355–376. https://doi.org/10.1016/j.jsames.2018.12.024.

Armendáriz, M., Rosales, I., Bádenas, B., Aurell, M., García-Ramos, J.C., Piñuela, L., 2012. High-resolution chemostratigraphic records from Lower Pliensbachian belemnites: Palaeoclimatic perturbations, organic facies and water mass exchange (Asturian basin, northern Spain). Palaeogeogr. Palaeoclimatol. Palaeoecol. 333, 178–191.

Baghli, H., Mattioli, E., Spangenberg, J.E., Bensalah, M., Arnaud-Godet, F., Pittet, B., Suan, G., 2020. Early Jurassic climatic trends in the south-Tethyan margin. Gondwana Res. 77, 67–81.

Bailey, T.R., Rosenthal, Y., McArthur, J.M., Van de Schootbrugge, B., Thirlwall, M.F., 2003. Paleoceanographic changes of the Late Pliensbachian–Early Toarcian interval: a possible link to the genesis of an Oceanic Anoxic Event. Earth Planet. Sci. Lett. 212 (3–4), 307–320. https://doi.org/10.1016/S0012-821X(03)00278-4.

Bamford, M.K., 2004. Diversity of the woody vegetation of Gondwanan Southern Africa. Gondwana Res. 7 (1), 153–164.

Basilici, G., Mesquita, Á.F., Soares, M.V.T., Janočko, J., Mountney, N.P., Colombera, L., 2021. A Mesoproterozoic hybrid dry-wet aeolian system: Galho do Miguel Formation, SE Brazil. Precambrian Res. 359, 106216. https://doi.org/10.1016/j.precamres.2021.106216.

Benavente, C.A., Bohacs, K.M., 2024. Advances in Limnology: the lake-basin-type model revisited 25 years after…anomalies, conundrums and upgrades. Depositional Rec. 10, 748–792. https://doi.org/10.1002/dep2.280.

Beukes, N.J., 1969. Die sedimentologie van die Etage Holkranssandsteen, sisteem Karoo. Unpublished MSc dissertation. University of the Orange Free State, Bloemfontein, p. 138. Available: http://hdl.handle.net/11660/7671.

Beukes, N.J., 1970. Stratigraphy and sedimentology of the Cave Sandstone stage, Karoo System. In: Haughton, S.H. (Ed.), Proceedings and Papers of the 2nd Gondwana Symposium. Council for Scientific and Industrial Research, Pretoria, pp. 321–341.

Bivand, R.S., Pebesma, E., Gómez-Rubio, V., 2013. Interpolation and geostatistics. In *Applied spatial data analysis with R* (pp. 213-261). Springer New York, New York, NY:

Bordy, E.M., 2008. Enigmatic trace fossils from the aeolian Lower Jurassic Clarens Formation, southern Africa. Palaeontol. Electron. 11, 16A.

Bordy, E.M., Catuneanu, O., 2001. Sedimentology of the upper Karoo fluvial strata in the Tuli Basin, South Africa. J. Afr. Earth Sci. 33 (3–4), 605–629. https://doi.org/10.1016/S0899-5362(01)00090-2.

Bordy, E.M., Head, H.V., 2018. Lithostratigraphy of the Clarens Formation (Stormberg Group, Karoo Supergroup), South Africa. S. Afr. J. Geol. 121, 119–130. https://doi.org/10.25131/sajg.121.0009.

Bordy, E.M., Catuneanu, O., 2002. Sedimentology and palaeontology of upper Karoo aeolian strata (Early Jurassic) in the Tuli Basin, South Africa. J. Afr. Earth Sci. 35, 301–314.

Bordy, E.M., Hancox, P.J., Rubidge, B.S., 2004a. Basin development during the deposition of the Elliot Formation (Late Triassic-Early Jurassic), Karoo Supergroup, South Africa. S. Afr. J. Geol. 107 (3), 397–412. https://doi.org/10.2113/107.3.397.

Bordy, E.M., Hancox, P.J., Rubidge, B.S., 2004b. Fluvial style variations in the Late Triassic–Early Jurassic Elliot Formation, main Karoo Basin, South Africa. J. Afr. Earth Sci. 38 (4), 383–400. https://doi.org/10.1016/j.jafrearsci.2004.02.004.

Bordy, E.M., Hancox, P.J., Rubidge, B.S., 2005. The contact of the Molteno and Elliot formations through the main Karoo Basin, South Africa: a second-order sequence boundary. S. Afr. J. Geol. 108 (3), 351–364. https://doi.org/10.2113/108.3.351.

Bordy, E.M., Rampersadh, A., Abrahams, M., Lockley, M.G., Head, H.V., 2020. Tracking the Pliensbachian–Toarcian Karoo firewalkers: trackways of quadruped and biped dinosaurs and mammaliaforms. PLoS One 15 (1), e0226847. https://doi.org/10.1371/journal.pone.0226847.

Bordy, E.M., Haupt, T.N., Head, H.V., 2021. Karoo lava-fed deltas and a petrified forest from the Lower Jurassic of southern Gondwana. Palaeogeogr. Palaeoclimatol. Palaeoecol. 575, 110484. https://doi.org/10.1016/j.palaeo.2021.110484.

Bordy, E.M., Lockley, M.G., Rampersadh, A., Mukaddam, R., Head, H.V., 2023. Life and land engulfed in the Late Early Jurassic Karoo lavas of southern Gondwana. Geol. Mag. 160 (4), 535–666.

Broom, R., 1904. On a new crocodilian genus (Notochampsa) from the Upper Stormberg beds of South Africa. Geol. Mag. 1, 582–584.

Cain, S.A., Mountney, N.P., 2009. Spatial and temporal evolution of a terminal fluvial fan system: the Permian Organ Rock Formation, South-east Utah, USA. Sedimentology 56 (6), 1774–1800. https://doi.org/10.1111/j.1365-3091.2009.01057.x.

Catuneanu, O., Hancox, P.J., Rubidge, B.S., 1998. Reciprocal flexural behaviour and contrasting stratigraphies: a new basin development model for the Karoo retroarc foreland system, South Africa. Basin Res. 10 (4), 417–440. https://doi.org/10.1046/j.1365-2117.1998.00078.x.

Catuneanu, O., Wopfner, H., Eriksson, P.G., Cairncross, B., Rubidge, B.S., Smith, R.M.H., Hancox, P.J., 2005. The Karoo basins of south-Central Africa. J. Afr. Earth Sci. 43 (1–3), 211–253. https://doi.org/10.1016/j.jafrearsci.2005.07.007.

Chandler, M.A., Rind, D., Ruedy, R., 1992. Pangaean climate during the Early Jurassic: GCM simulations and the sedimentary record of paleoclimate. Geol. Soc. Am. Bull. 104 (5), 543–559. https://doi.org/10.1130/0016-7606(1992)104<0543:PCDTEJ>2.3.CO;2.

Cole, D.I., 1992. Evolution and development of the Karoo Basin. In: De Wit, M.J., Ransome, I.G.D. (Eds.), Inversion Tectonics of the Cape Fold Belt, Karoo and Cretaceous Basins of Southern Africa. Balkema, Rotterdam, The Netherlands, pp. 87–99.

Cosgrove, G.I., Alkathery, M., Al-Masrahy, M., Colombera, L., Mountney, N.P., Thompson, D.B., 2025. Quantitative Sedimentological Analysis of the Aeolian–Fluvial Triassic Sherwood Sandstone Group. Sedimentology, Cheshire Basin, UK. https://doi.org/10.1111/sed.70000.

Cosgrove, G.I.E., Colombera, L., Mountney, N.P., 2021a. Quantitative analysis of the sedimentary architecture of eolian successions developed under icehouse and greenhouse climatic conditions. GSA Bull. https://doi.org/10.1130/B35918.1.

Cosgrove, G.I.E., Colombera, L., Mountney, N.P., 2021b. A database of Aeolian Sedimentary Architecture for the characterization of modern and ancient sedimentary systems. Mar. Pet. Geol. 127, 104983. https://doi.org/10.1016/j.marpetgeo.2021.104983.

Cosgrove, G.I.E., Colombera, L., Mountney, N.P., 2022. The role of subsidence and accommodation generation in controlling the nature of the aeolian stratigraphic record. J. Geol. Soc. Lond. 179 (1) pp.jgs2021-042.

Crabaugh, M., Kocurek, G., 1993. Entrada Sandstone: an example of a wet aeolian system. Geol. Soc. Lond. Spec. Publ. 72 (1), 103–126. https://doi.org/10.1144/GSL.SP.1993.072.01.11.

Dasgupta, P., 2002. Determination of paleocurrent direction from oblique sections of trough cross-stratification—A precise approach. J. Sediment. Res. 72, 217–219. https://doi.org/10.1306/050401720217.

Dera, G., Brigaud, B., Monna, F., Laffont, R., Pucéat, E., Deconinck, J.F., Pellenard, P., Joachimski, M.M., Durlet, C., 2011. Climatic ups and downs in a disturbed Jurassic world. Geology 39 (3), 215–218. https://doi.org/10.1130/G31579.1.

van Dijk, D.E., Eriksson, P.G., 2021. Bipedal leaping Jurassic vertebrates in Southern Africa: proposed new ichnotaxon and inferred palaeoenvironment. Trans. R. Soc. S. Afr. 76 (3), 235–245. https://doi.org/10.1080/0035919X.2021.1964104.

Dollman, K.N., Clark, J.M., Viglietti, P.A., Browning, C., Choiniere, J.N., 2021. Revised anatomy, taxonomy and biostratigraphy of Notochampsa istedana Broom, 1904, a Lower Jurassic crocodyliform from the Clarens Formation (Stormberg Group), and its implications for early crocodyliform phylogeny. J. Syst. Palaeontol. 1–25. https://doi.org/10.1080/14772019.2021.1948926.

Du Toit, A.L., 1904. Geological survey of the divisions of Elliot and Xalanga, Tembuland. Ann. Report Geol. Comm. Cape Good Hope 1903, 169–205.

Du Toit, A.L., 1905. Geological survey of the division of Aliwal North, Herschel, Barkly East and part of Wodehouse: Annual Report of the Geological Commission of the Cape of Good Hope., pp. 71–181.

Du Toit, A.L., 1910. Geological survey of Maclear and portions of Engcobo, Mount Fletcher, Qumbu and Mount Frere. Annual Report of the Geological Commission of the Cape of Good Hope, pp. 69–108.

Du Toit, A.L., 1918. The zones of the Karroo System and their distribution. Proceed. Geol. Soc. S. Afr. 21, 17–36.

Duncan, R.A., Hooper, P.R., Rehacek, J., Marsh, J.S., Duncan, A.R., 1997. The timing and duration of the Karoo igneous event, southern Gondwana. J. Geophys. Res. 102, 18127–18138. https://doi.org/10.1029/97JB00972.

Eriksson, P.G., 1979. Mesozoic sheetflow and playa sediments of the Clarens Formation in the Kamberg area of the Natal Drakensberg. S. Afr. J. Geol. 82 (2), 257–258.

Eriksson, P.G., 1981. A palaeoenvironmental analysis of the Clarens Formation in the Natal Drakensberg. Transact. Geol. Soc. S. Afr. 84, 7–17.

Eriksson, P.G., 1983. A Palaeoenvironmental Study of the Molteno, Elliot and Clarens Formations in the Natal Drakensberg and Northeastern Orange Free State. Unpublished doctoral dissertation. University of Natal, Pietermaritzburg.

Eriksson, P.G., 1986. Aeolian dune and alluvial fan deposits in the Clarens Formation of the Natal Drakensberg. Transact. Geol. Soc. S. Afr. 89, 389–393.

Fitzsimmons, K.E., Cohen, T.J., Hesse, P.P., Jansen, J., Nanson, G.C., May, J.H., Barrows, T.T., Haberlah, D., Hilgers, A., Kelly, T., Larsen, J., 2013. Late Quaternary palaeoenvironmental change in the Australian drylands. Quat. Sci. Rev. 74, 78–96.

Forey, P., Gardiner, B.G., 1973. A new dictyopygid from the Cave Sandstone of Lesotho, Southern Africa. Palaeontol. Afr. 15, 29–31.

Gómez, J.J., Comas-Rengifo, M.J., Goy, A., 2016. Palaeoclimatic oscillations in the Pliensbachian (Early Jurassic) of the Asturian Basin (northern Spain). Clim. Past 12 (5), 1199–1214.

Gómez, J.J., Goy, A., Canales, M.L., 2008. Seawater temperature and carbon isotope variations in belemnites linked to mass extinction during the Toarcian (Early Jurassic) in Central and Northern Spain. Comparison with other European sections. Palaeogeogr. Palaeoclimatol. Palaeoecol. 258 (1–2), 28–58. https://doi.org/10.1016/j.palaeo.2007.11.005.

Goudie, A.S., 2013. Arid and Semi-Arid Geomorphology. Cambridge University Press, p. 454.

Hampton, B.A., Horton, B.K., 2007. Sheetflow fluvial processes in a rapidly subsiding basin, Altiplano plateau, Bolivia. Sedimentology 54 (5), 1121–1148. https://doi.org/10.1111/j.1365-3091.2007.00875.x.

Hancox, P.J., 1998. A stratigraphic, sedimentological and palaeonviron-mental synthesis of the Beaufort-Molteno contact in the Karoo Basin. In: Unpublished Doctoral Dissertation. University of the Witwatersrand, Johannesburg, South Africa.

Hanson, E.K., Moore, J.M., Bordy, E.M., Marsh, J.S., Howarth, G., Robey, J.V.A., 2009. Cretaceous erosion in Central South Africa: evidence from upper-crustal xenoliths in kimberlite diatremes. S. Afr. J. Geol. 112 (2), 125–140. https://doi.org/10.2113/gssajg.112.2.125.

Harazim, D., Van De Schootbrugge, B.A.S., Sorichter, K., Fiebig, J., Weug, A., Suan, G., Oschmann, W., 2013. Spatial variability of watermass conditions within the European Epicontinental Seaway during the Early Jurassic (Pliensbachian–Toarcian). Sedimentology 60 (2), 359–390. https://doi.org/10.1111/j.1365-3091.2012.01344.x.

Hassan, M.S., Venetikidis, A., Bryant, G. and Miall, A.D. 2018. The sedimentology of an ERG margin: the Kayenta–Navajo transition (Lower Jurassic), Kanab, Utah, USA. J. Sediment. Res., 88(5): 613–640. DOI: doi: https://doi.org/10.2110/jsr.2018.31.

Hasiotis, S.T., Chan, M.A., Parrish, J.T., 2021. Defining bounding surfaces within and between eolian and non-eolian deposits, Lower Jurassic Navajo Sandstone, Moab Area, Utah, USA: Implications for subdividing erg system strata. J. Sed. Res. 91 (12), 1275–1304.

Haughton, S.H., 1924. The Fauna and stratigraphy of the Stormberg Series. Ann. S. Afr. Museum 8, 1–517.

Haupt, T., 2018. Palaeoenvironmental Change from the Hettangian to Toarcian in Moyeni (Quthing District), Southwestern Lesotho. Unpublished MSc dissertation. University of Cape Town, p. 112. Available: http://hdl.handle.net/11427/30021.

Head, H.V., 2022. The Karoo sand sea in changing climates: Early Jurassic interdune lakes and erg dynamics in southern Africa. Unpublished PhD thesis. University of Cape Town, p. 205. http://hdl.handle.net/11427/36918.

Head, H.V., Bordy, E.M., 2023a. Lake dynamics in an Early Jurassic desert: evidence from the Clarens Formation in southern Africa. Sedimentology 70 (3), 865–894.

Head, H.V., Bordy, E.M., 2023b. Loess or lake sediments: Resolving the origin of massive beds in the Lower Jurassic of southern Africa. Geol. J. 58 (5), 1822–1843.

Head, H.V., Bordy, E.M., Bolhar, R., 2024. Sedimentation tempo in an Early Jurassic erg system: Refined chronostratigraphy and provenance of the Clarens Formation of southern Africa. Basin Res. 36 (3), e12877.

Hême de Lacotte, V.J.P., Mountney, N.P., 2022. A classification scheme for sedimentary architectures arising from aeolian-fluvial system interactions: Permian examples from Southeast Utah, USA. Aeolian Res. 58, 100815. https://doi.org/10.1016/j.aeolia.2022.100815.

Heness, E.A., Simpson, E.L., Bumby, A.J., Eriksson, P.G., Eriksson, K.A., Hilbert-Wolf, H. L., Okafor, O.J., Linnevelt, S., Malenda, H.F., Modungwa, T., 2014. Evidence for climate shifts in the $\sim$ 2.0 Ga upper Makgabeng Formation erg, South Africa. Palaeogeogr. Palaeoclimatol. Palaeoecol. 409, 265–279. https://doi.org/10.1016/j.palaeo.2014.05.016.

Hesselbo, S.P., Gröcke, D.R., Jenkyns, H.C., Bjerrum, C.J., Farrimond, P., Bell, H.S.M., Green, O.R., 2000. Massive dissociation of gas hydrate during a Jurassic oceanic anoxic event. Nature 406 (6794), 392–395. https://doi.org/10.1038/35019044.

High, L.R., Picard, M.D., 1974. Reliability of cross-stratification types as paleocurrent indicators in fluvial rocks. J. Sediment. Res. 44, 158–168. https://doi.org/10.1306/74D729AF-2B21-11D7-8648000102C1865D.

Holzförster, F., 2007. Lithology and depositional environments of the Lower Jurassic Clarens Formation in the eastern Cape, South Africa. S. Afr. J. Geol. 110 (4), 543–560. https://doi.org/10.2113/gssajg.110.4.543.

Holzförster, F., Stollhofen, H., Stanistreet, I.G., 1999. Lithostratigraphy and depositional environments in the Waterberg-Erongo area, Central Namibia, and correlation with the main Karoo Basin, South Africa. J. Afr. Earth Sci. 29 (1), 105–123. https://doi.org/10.1016/S0899-5362(99)00083-4.

Hummel, G., Kocurek, G., 1984. Interdune areas of the back-island dune field, North Padre Island, Texas. Sediment. Geol. 39 (1–2), 1–26. https://doi.org/10.1016/0037-0738(84)90022-8.

Hunter, R.E., 1977. Basic types of stratification in small eolian dunes. Sedimentology 24, 361–387. https://doi.org/10.1111/j.1365-3091.1977.tb00128.x.

Hunter, R.E., 1981. Stratification styles in eolian sandstones: some Pennsylvanian to Jurassic examples from the western interior USA. SEPM Spec. Public. 31, 315–329.

Jenkyns, H.C., Jones, C.E., Gröcke, D.R., Hesselbo, S.P., Parkinson, D.N., 2002. Chemostratigraphy of the Jurassic System: applications, limitations and implications for palaeoceanography. J. Geol. Soc. Lond. 159 (4), 351–378. https://doi.org/10.1144/0016-764901-130.

Jerram, D.A., Stollhofen, H., 2002. Lava–sediment interaction in desert settings; are all peperite-like textures the result of magma–water interaction? J. Volcanol. Geotherm. Res. 114 (1–2), 231–249. https://doi.org/10.1016/S0377-0273(01)00279-7.

Jerram, D.A., Mountney, N., Stollhofen, H., 1999. Facies architecture of the Etjo Sandstone Formation and its interaction with the basal Etendeka Flood Basalts of Northwest Namibia: implications for offshore prospectivity. Geol. Soc. Lond. Spec. Publ. 153 (1), 367–380. https://doi.org/10.1144/GSL.SP.1999.153.01.22.

Jerram, D.A., Mountney, N.P., Howell, J.A., Long, D., Stollhofen, H., 2000. Death of a sand sea: an active aeolian erg systematically buried by the Etendeka flood basalts of NW Namibia. J. Geol. Soc. Lond. 157 (3), 513–516. https://doi.org/10.1144/jgs.157.3.513.

Johnson, M.R., 1976. Stratigraphy and Sedimentology of the Cape and Karoo Sequences in the Eastern Cape Province. Unpublished doctoral dissertation. Rhodes University, Grahamstown, South Africa, p. 336. Available at http://hdl.handle.net/10962/d1005617.

Johnson, M.R., Van Vuuren, C.J., Hegenberger, W.F., Key, R., Shoko, U., 1996. Stratigraphy of the Karoo Supergroup in southern Africa: an overview. J. Afr. Earth Sci. 23, 3–15. https://doi.org/10.1016/S0899-5362(96)00048-6.

Jubb, R.A., 1973. Brief synthesis of present information on the geographical and stratigraphical distribution of fossil fish within the Stormberg Series, South Africa. Palaeontol. Afr. 16, 17–23.

Kocurek, G., 1991. Interpretation of ancient eolian sand dunes. Annu. Rev. Earth Planet. Sci. 19, 43–75. https://doi.org/10.1146/annurev.ea.19.050191.000355.

Kocurek, G., 2003. Limits on extreme eolian systems: Sahara of Mauritania and Jurassic Navajo Sandstone examples. In: Chan, M., Archer, A.W. (Eds.), Extreme Depositional Environments: Mega End Members in Geologic Time, GSA Special Paper, vol. 370, pp. 43–52. https://doi.org/10.1130/0-8137-2370-1.43.

Kocurek, G., Day, M., 2018. What is preserved in the aeolian rock record? A Jurassic Entrada Sandstone case study at the Utah–Arizona border. Sedimentology 65 (4), 1301–1321. https://doi.org/10.1111/sed.12422.

Kocurek, G., Dott, R.H., 1981. Distinction and uses of stratification types in the interpretation of eolian sand. J. Sediment. Petrol. 51, 579–595. https://doi.org/10.1306/212F7CE3-2B24-11D7-8648000102C1865D.

Kocurek, G., Havholm, K.G., 1993. Eolian Sequence Stratigraphy – conceptual framework. In: Weimer, P., Posamentier, H.W. (Eds.), Recent Developments in Siliciclastic Sequence Stratigraphy, 58. American Association of Petroleum Geologists, Memoir, pp. 393–409.

Kocurek, G., Nielson, J., 1986. Conditions favourable for the formation of warm-climate aeolian sand sheets. Sedimentology 33 (6), 795–816. https://doi.org/10.1111/j.1365-3091.1986.tb00983.x.

Korte, C., Hesselbo, S.P., 2011. Shallow marine carbon and oxygen isotope and elemental records indicate icehouse-greenhouse cycles during the Early Jurassic. Paleoceanography 26 (4), PA4219. https://doi.org/10.1029/2011PA002160.

Korte, C., Hesselbo, S.P., Ullmann, C.V., Dietl, G., Ruhl, M., Schweigert, G., Thibault, N., 2015. Jurassic climate mode governed by ocean gateway. Nat. Commun. 6 (1), 10015.

Kutzbach, J.E., 1994. Idealized Pangean climates: sensitivity to orbital change. Geol. Soc. Am. Spec. Pap. 288, 41–56.

Kutzbach, J.E., Gallimore, R.G., 1989. Pangaean climates: megamonsoons of the megacontinent. J. Geophys. Res. Atmos. 94 (D3), 3341–3357. https://doi.org/10.1029/JD094iD03p03341.

Langford, R.P., Chan, M.A., 1989. Fluvial-aeolian interactions: Part II, ancient systems. *Sedimentology* 36 (6), 1037–1051. https://doi.org/10.1111/j.1365-3091.1989.tb01541.x.

Langford, R.P., Chan, M.A., 1993. Downwind changes within an ancient dune sea, Permian Cedar Mesa Sandstone, Southeast Utah. In: Pye, K., Lancaster, N. (Eds.), Aeolian Sediments: Ancient and Modern. International Association of Sedimentologists, pp. 109–126. https://doi.org/10.1002/9781444303971.ch8.

Li, Q., McArthur, J.M., Atkinson, T.C., 2012. Lower Jurassic belemnites as indicators of palaeo-temperature. Palaeogeogr. Palaeoclimatol. Palaeoecol. 315, 38–45. https://doi.org/10.1016/j.palaeo.2011.11.006.

Lock, B.E., Paverd, A.L., Broderick, T.J., 1974. Stratigraphy of the Karoo volcanic rocks of the Barkly East district. Transact. Geol. Soc. S. Afr. 77, 177–129.

Long, H., Lai, Z., Fuchs, M., Zhang, J., Yang, L., 2012. Palaeodunes intercalated in loess strata from the western Chinese Loess Plateau: Timing and palaeoclimatic implications. Quatern. Int. 263, 37–45.

Loope, D.B., Dingus, L., Swisher III, C.C., Minjin, C., 1998. Life and death in a Late Cretaceous dune field, Nemegt basin, Mongolia. Geology 26, 27–30. https://doi.org/10.1130/0091-7613(1998)026<0027:LADIAL>2.3.CO;2.

Loope, D.B., Rowe, C.M., Joeckel, R.M., 2001. Annual monsoon rains recorded by Jurassic dunes. Nature 412 (6842), 64–66. https://doi.org/10.1038/35083554.

Loope, D.B., Steiner, M.B., Rowe, C.M., Lancaster, N., 2004. Tropical westerlies over Pangaean sand seas. Sedimentology 51 (2), 315–322. https://doi.org/10.1046/j.1365-3091.2003.00623.x.

Marsh, J.S., Eales, H.V., 1984. The chemistry and petrogenesis of igneous rocks of the Karoo central area, Southern Africa. In: Erlank, A.J. (Ed.), Petrogenesis of the Volcanic Rocks of the Karoo Province. Geological Society of South Africa, Special Publication, vol. 13, pp. 27–67.

McArthur, J.M., Donovan, D.T., Thirlwall, M.F., Fouke, B.W., Mattey, D., 2000. Strontium isotope profile of the early Toarcian (Jurassic) oceanic anoxic event, the duration of ammonite biozones, and belemnite palaeotemperatures. Earth Planet. Sci. Lett. 179 (2), 269–285. https://doi.org/10.1016/S0012-821X(00)00111-4.

McClintock, M., Marsh, J.S., White, J.D., 2008. Compositionally diverse magmas erupted close together in space and time within a Karoo flood basalt crater complex. Bull. Volcanol. 70 (8), 923–946. https://doi.org/10.1007/s00445-007-0178-6.

McKee, E.D., 1966. Structures of dunes at White Sands National Monument, New Mexico (and a comparison with structures of dunes from other selected areas). Sedimentology 7, 1–69. https://doi.org/10.1111/j.1365-3091.1966.tb01579.x.

Meijs, L., 1960. Notes on the Occurrence of Petrified Wood in Basutoland. Pius XII University Collage, Roma, Basutoland, p. 8. Papers No. 2.

Miall, A.D., 1974. Paleocurrent analysis of alluvial sediments; a discussion of directional variance and vector magnitude. J. Sediment. Res. 44, 1174–1185. https://doi.org/10.1306/212F6C6C-2B24-11D7-8648000102C1865D.

Miall, A.D., 1985. Architectural-element analysis: a new method of facies analysis applied to fluvial deposits. Earth Sci. Rev. 22 (4), 261–308. https://doi.org/10.1016/0012-8252(85)90001-7.

Miall, A.D., 1996. Geology of Fluvial Deposits. Springer-Verlag, Berlin, p. 582.

Miall, A.D., 2016. Stratigraphy: A Modern Synthesis. Springer-Verlag, Berlin, p. 454.

Moulin, M., Fluteau, F., Courtillot, V., Marsh, J., Delpech, G., Quidelleur, X., Gérard, M., Jay, A.E., 2011. An attempt to constrain the age, duration, and eruptive history of the Karoo flood basalt: Naude's Nek section (South Africa). J. Geophys. Res. Solid Earth 116 (B07403). https://doi.org/10.1029/2011JB008210.

Moulin, M., Fluteau, F., Courtillot, V., Marsh, J., Delpech, G., Quidelleur, X., Gérard, M., 2017. Eruptive history of the Karoo lava flows and their impact on Early Jurassic environmental change. J. Geophys. Res. Solid Earth 122 (2), 738–772. https://doi.org/10.1002/2016JB013354.

Mountney, N.P., Mountney, N.P., Posamentier, H.W., Walker, R.G., 2006. Eolian facies models. In: Facies Models Revisited, 84. SEPM Special Publication, pp. 19–83. https://doi.org/10.2110/pec.06.84.0019.

Mountney, N.P., Howell, J., 2000. Aeolian architecture, bedform climbing and preservation space in the Cretaceous Etjo Formation, NW Namibia. Sedimentology 47 (4), 825–849.

Mountney, N.P., Jagger, A., 2004. Stratigraphic evolution of an aeolian erg margin system: the Permian Cedar Mesa Sandstone, SE Utah, USA. Sedimentology 52, 713–743. https://doi.org/10.1111/j.1365-3091.2004.00646.x.

Mountney, N.P., Thompson, D.B., 2002. Stratigraphic evolution and preservation of aeolian dine and damp/wet interdune strata: an example from the Triassic Helsby Sandstone Formation, Cheshire Basin, UK. Sedimentology 49, 805–833. https://doi.org/10.1046/j.1365-3091.2002.00472.x.

Muhs, D.R., Bettis, A.E., 2003. Quaternary loess-paleosol sequences as examples of climate-driven sedimentary extremes. Geol. Soc. Am. Spec. Pap. 370, 53–74.

Muir, R.A., Bordy, E.M., Mundil, R., Frei, D., 2020. Recalibrating the breakup history of SW Gondwana: U–Pb radioisotopic age constraints from the southern Cape of South Africa. Gondwana Res. 84, 177–193. https://doi.org/10.1016/j.gr.2020.02.011.

Neuman, C.M., Scott, M.M., 1998. A wind tunnel study of the influence of pore water on aeolian sediment transport. J. Arid Environ. 39 (3), 403–419. https://doi.org/10.1006/jare.1997.0371.

North, C.P., Davidson, S.K., 2012. Unconfined alluvial flow processes: recognition and interpretation of their deposits, and the significance for palaeogeographic reconstruction. Earth Sci. Rev. 111 (1–2), 199–223. https://doi.org/10.1016/j.earscirev.2011.11.008.

Parrish, J.T., Peterson, F., 1988. Wind directions predicted from global circulation models and wind directions determined from eolian sandstones of the western United States—A comparison. Sediment. Geol. 56 (1–4), 261–282. https://doi.org/10.1016/0037-0738(88)90056-5.

Pebesma, E.J., 2004. Multivariable geostatistics in S: the gstat package. Comput. Geosci. 30, 683–691. https://doi.org/10.1016/j.cageo.2004.03.012.

Pebesma, E.J., Bivand, R.S., 2005. Classes and methods for spatial data in R. R News 5 (2). https://cran.r-project.org/doc/Rnews/.

Pérez Mayoral, J., Argüello Scotti, A., Apesteguía, S., Veiga, G.D., 2021. High-resolution analysis of an erg-margin system from the Cretaceous Candeleros Formation (La Buitrera Paleontological Area, Río Negro Province, Argentina): An approach to different scales of fluvial-aeolian interactions. Lat. Am. J. Sedimentol. Basin Anal. 28 (1), 37–60.

Petry, K., Jerram, D.A., Delia del Pilar, M., Zerfass, H., 2007. Volcanic-sedimentary features in the Serra Geral Fm., Paraná Basin, southern Brazil: examples of dynamic lava-sediment interactions in an arid setting. J. Volcanol. Geotherm. Res. 159 (4), 313–325. https://doi.org/10.1016/j.jvolgeores.2006.06.017.

Porter, M.L., 1986. Sedimentary record of erg migration. Geology 14 (6), 497–500. https://doi.org/10.1130/0091-7613(1986)14<497:SROEM>2.0.CO;2.

Porter, M.L., 1987. Sedimentology of an ancient erg margin: the Lower Jurassic Aztec Sandstone, southern Nevada and southern California. Sedimentology 34 (4), 661–680. https://doi.org/10.1111/j.1365-3091.1987.tb00793.x.

Porter, S.C., Zhisheng, A., 1995. Correlation between climate events in the North Atlantic and China during the last glaciation. Nature 375 (6529), 305–308.

Price, G.D., 1999. The evidence and implications of polar ice during the Mesozoic. Earth Sci. Rev. 48 (3), 183–210. https://doi.org/10.1016/S0012-8252(99)00048-3.

Priddy, C.L., Clarke, S.M., 2020. The sedimentology of an ephemeral fluvial–aeolian succession. Sedimentology 67 (5), 2392–2425. https://doi.org/10.1111/sed.12706.

Pye, K., 1995. The nature, origin and accumulation of loess. Quat. Sci. Rev. 14, 653–667. https://doi.org/10.1016/0277-3791(95)00047-X eolian.

R Core Team, 2014. R: A Language and Environment for Statistical Computing. R Foundation for Statistical Computing, Vienna, Austria. Available: http://www.R-project.org/.

Rampersadh, A., Bordy, E.M., Sciscio, L., Abrahams, M., 2018. Dinosaur behaviour in an Early Jurassic palaeoecosystem–uppermost Elliot Formation, Ha Nohana, Lesotho. Ann. Soc. Geol. Pol. 88, 163–179. https://doi.org/10.14241/asgp.2018.010.

Robinson, D.N., Beer, H.M., Nutsch, F.M., Trumpelman, F., 1969. The Geology and Oil Potential of the Stormberg Group. Unpublished report. Southern Oil Exploration Corporation, Johannesburg.

Rosales, I., Quesada, S., Robles, S., 2004. Paleotemperature variations of Early Jurassic seawater recorded in geochemical trends of belemnites from the Basque–Cantabrian basin, northern Spain. Palaeogeogr. Palaeoclimatol. Palaeoecol. 203 (3–4), 253–275. https://doi.org/10.1016/S0031-0182(03)00686-2.

Rubin, D.M., Hunter, R.E., 1982. Bedform climbing in theory and nature. Sedimentology 29, 121–138. https://doi.org/10.1111/j.1365-3091.1982.tb01714.x.

Scherer, C.M., Goldberg, K., 2010. Cyclic cross-bedding in the eolian dunes of the Sergi Formation (Upper Jurassic), Recôncavo Basin: inferences about the wind regime. Palaeogeogr. Palaeoclimatol. Palaeoecol. 296 (1–2), 103–110. https://doi.org/10.1016/j.palaeo.2010.06.018.

Scherer, C.M., Lavina, E.L., 2005. Sedimentary cycles and facies architecture of aeolian–fluvial strata of the Upper Jurassic Guará Formation, Southern Brazil. Sedimentology 52 (6), 1323–1341. https://doi.org/10.1111/j.1365-3091.2005.00746.x.

Schmitz, G., Rooyani, F., 1987. Lesotho: Geology, Geomorphology, Soils. National University of Lesotho, p. 204.

Sciscio, L., de Kock, M., Bordy, E.M., Knoll, F., 2017. Magnetostratigraphy across the Triassic-Jurassic boundary in the main Karoo Basin. Gondwana Res. 51, 177–192. https://doi.org/10.1016/j.gr.2017.07.009.

Scotese, C.R., Boucot, A.J., McKerrow, W.S., 1999. Gondwanan palaeogeography and pal1 oclimatology. J. Afr. Earth Sci. 28 (1), 99–114. https://doi.org/10.1016/S0899-5362(98)00084-0.

Selker, J.S., 1993. Expressions for the formation of load casts in soft sediment. J. Sediment. Res. 63 (6), 1149–1151. https://doi.org/10.1306/D4267CCB-2B26-11D7-8648000102C1865D.

Simpson, E.L., Eriksson, K.A., Eriksson, P.A., Bumby, A.J., 2002. Eolian dune degradation and generation of massive sandstone bodies in the Paleoproterozoic Makgabeng Formation, Waterberg Group, South Africa. J. Sediment. Res. 72, 40–45. https://doi.org/10.1306/050701720040.

Skinner, E.M.W., Clement, C.R., Gurney, D.B., Apter, D.B., Hatton, C.J., 1992. The distribution and tectonic setting of South-African Kimberlites. Russ. Geol. Geophys. 33 (10), 26–31.

Stockley, G.M., 1947. The Geology of Basutoland. Geol. Mag. 77 (6), 444–460. https://doi.org/10.1017/S0016756800071600.

Suan, G., Mattioli, E., Pittet, B., Mailliot, S., Lécuyer, C., 2008. Evidence for major environmental perturbation prior to and during the Toarcian (Early Jurassic) oceanic anoxic event from the Lusitanian Basin, Portugal. Paleoceanography 23 (1), PA1202. https://doi.org/10.1029/2007PA001459.

Svendsen, J., Stollhofen, H., Krapf, C.B., Stanistreet, I.G., 2003. Mass and hyperconcentrated flow deposits record dune damming and catastrophic breakthrough of ephemeral rivers, Skeleton Coast Erg, Namibia. Sediment. Geol. 160, 7–31. https://doi.org/10.1016/S0037-0738(02)00334-2.

Svensen, H., Corfu, F., Polteau, S., Hammer, Ø., Planke, S., 2012. Rapid magma emplacement in the Karoo large igneous province. Earth Planet. Sci. Lett. 325, 1–9.

Sweeney, M.R., Loope, D.B., 2001. Holocene dune-sourced alluvial fans in the Nebraska Sand Hills. Geomorphology 38, 31–46. https://doi.org/10.1016/S0169-555X(00)00067-2.

Trewin, N.H., 1993. Mixed aeolian sand sheet and fluvial deposits in the Tumblagooda Sandstone, Western Australia. Geol. Soc. Lond. Spec. Publ. 73 (1), 219–230. https://doi.org/10.1144/GSL.SP.1993.073.01.13.

Van de Schootbrugge, B., Bailey, T.R., Rosenthal, Y., Katz, M.E., Wright, J.D., Miller, K. G., Feist-Burkhardt, S., Falkowski, P.G., 2005. Early Jurassic climate change and the radiation of organic-walled phytoplankton in the Tethys Ocean. Paleobiology 31 (1), 73–97. https://doi.org/10.1666/0094-8373(2005)031<0073:EJCCAT>2.0.CO;2.

Van Eeden, O.R., 1937. The geology of the country around Bethlehem and Kestell, with special reference to oil indications. Memoir. Geol. Surv. S. Afr. 33, 68.

Vandenberghe, J., 2013. Grain size of fine-grained windblown sediment: A powerful proxy for process identification. Earth Sci. Rev. 121, 18–30. https://doi.org/10.1016/j.earscirev.2013.03.001.

Vandenberghe, J., Sun, Y., Wang, X., Abels, H.A., Liu, X., 2018. Grain-size characterization of reworked fine-grained aeolian deposits. Earth Sci. Rev. 177, 43–52. https://doi.org/10.1016/j.earscirev.2017.11.005.

Veevers, J.J., 2004. Gondwanaland from 650–500 Ma assembly through 320 Ma merger in Pangea to 185–100 Ma breakup: supercontinental tectonics via stratigraphy and radiometric dating. Earth Sci. Rev. 68 (1–2), 1–132. https://doi.org/10.1016/j.earscirev.2004.05.002.

Veevers, J.J., Cole, D.I., Cowan, E.J., 1994. Southern Africa: Karoo Basin and Cape Fold Belt. Memoir of the Geological Society of America, pp. 184–223. https://doi.org/10.1130/MEM184-p223.